Marine and Petroleum Geology 167 (2024) 106913

Contents lists available at ScienceDirect

Marine and Petroleum Geology

journal homepage: www.elsevier.com/locate/marpetgeo

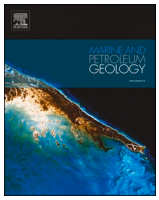

Unraveling the sediment routing systems evolution of the south Pyrenean foreland basin during the lower to middle Paleogene period

Philémon Juvany [a,b,*], Miguel Garcés [a,b], Miguel López-Blanco [a,b], Luís Valero [a,b], Elisabet Beamud Amorós [a,c], Miquel Poyatos-Moré [d], Albert Martínez Rius [e]

[a] Geomodels Research Institute, Universitat Barcelona, Facultat de Ciències de la Terra, Martí I Franquès s/n, 08028, Barcelona, Spain
[b] Departament de Dinàmica de la Terra I de l'Oceà, Universitat Barcelona, Facultat de Ciències de la Terra, Martí I Franquès s/n, 08028, Barcelona, Spain
[c] Paleomagnetic Laboratory CCiTUB-Geo3BCN(CSIC), Barcelona, Spain
[d] Departament de Geologia, Universitat Autònoma de Barcelona, Cerdanyola del Vallés, Spain
[e] Colegiado en el ICOG num. 242–Ilustrador científico, Experto en visualización de la información científica c/ Repartidor, 44 local 2, 08023, Barcelona, Spain

A B S T R A C T

Orogenesis plays a crucial role in creating, modifying, and disrupting sediment routing fairways. Reconstructing past source to sink systems is a critical step to unravel the geological history, mandatory to disentangle tectonic and climatic forcings, and to understand the perturbations that affected the overall system. The Paleocene-Eocene period is a debated early stage of the early Pyrenean orogeny, characterized by the piggy-back style tectonic partitioning of sub-basins as the deformation front propagates towards the southern foreland. An important issue is to understand how sedimentary systems reacted and reorganized in response to this dynamic scenario. and whether the stratigraphic and sediment provenance results align with the envisioned scenario.

In this paper we aim at contributing to the paleogeographic, sedimentologic and tectono-sedimentary evolution of the South-Pyrenean foreland basin by reviewing the chronostratigraphic framework of the basin infill in its south-central sector (the Ager sub-basin in the Serres Marginals thrust sheet). We built five new magnetostratigraphic sections, which together encompass most of the Paleogene record, aimed to best reconcile magnetostratigraphic data with the defined biostratigraphic framework of the region including marine Shallow Benthic Zones (SBZ biozones) and continental mammalian localities (MP levels). Detailed trends in subsidence show the development and evolution of the foreland depozones, from forebulge to foredeep and wedge-top setting, relative to the successive emplacement of the Montsec and Serres Marginals thrust sheets.

A correlation with the eastern portion of the foreland basin (Lower-Middle Pedraforca and Cadí Thrust Sheets) and adjacent northern Graus-Tremp basin (Montsec Thrust Sheet) was feasible and seeks to contribute to the tectono-sedimentary evolution of the South-Pyrenean foreland in the light of a source to sink approach. Our proposal includes a new paleogeographic evolution of the area in a series of paleogeographic maps from Late Thanetian to Late Cuisian times.

1. Introduction

Orogenic processes create vertical motions of the Earth surface, driving sediment erosion in regions subjected to uplift, and its transport to peripheral basins in subsiding regions. Sediments constitute the prime archive of the tectonic and climatic processes that shaped mountain belts. And a first critical step to read this record is to correctly frame the game board over which the surface processes operated and to reconstruct the sediment routing fairways. An accurate chronology helps establishing the correlation between the available discrete pieces and linking the different facies belts to understand the original sediment transfer system. A detailed chronostratigraphic framework is therefore crucial to elucidate the processes driving the foreland basin evolution at a mountain range scale.

The Paleocene-Eocene period corresponds to the early stage of growth of the Pyrenees, characterized in its southern side by thin-skinned thrust-tectonics leading to partitioning of the foreland into sub-basins (Garrido-Megias, 1973; Puigdefabregas, 1975; Puigdefàbregas and Souquet, 1986; Puigdefàbregas et al., 1992; Muñoz, 1992; Vergés, 1993; Teixell and Muñoz, 2000). As the deformation front propagated southwards in a piggy-back sequence, sediment transfer systems evolved and part of the distal sections (originally in the autochthonous foredeep) were progressively incorporated into the deformation of the fold-and-thrust belt (allochthonous wedge top). Understanding how sedimentary systems have responded and reorganized under these constraints is a crucial issue to assess the evolution of the system from a source-to-sink perspective. Integration of existing stratigraphic, sedimentologic, and sediment provenance data is required.

Our study focuses on the Ager sub-basin, an E-W trending syncline

* Corresponding author. Geomodels Research Institute, Universitat Barcelona, Facultat de Ciències de la Terra, Martí I Franquès s/n, 08028, Barcelona, Spain.
E-mail address: philemonjuvany@outlook.fr (P. Juvany).

https://doi.org/10.1016/j.marpetgeo.2024.106913
Received 3 January 2024; Received in revised form 20 May 2024; Accepted 26 May 2024
Available online 1 June 2024

located on top of one of the meridional thrust sheets of the south-central Pyrenean unit and whose present-day extension towards proximal and distal areas is hidden below unconformable younger strata. Due to this present-day limited extension, previous paleogeographic reconstructions of the Ager sub-basin in the South-Central Pyrenees showed contrasting interpretations. Some authors (Mutti et al., 1985; Dreyer and Fält, 1993; Martinius, 2012) show the Ager and Tremp sub-basins connected westwards to the sea and disconnected towards the eastern margin of the basin. On the other hand, Nijman (1998), Martinius (2012) and Olariu et al. (2012), suggest a marine connection towards the east. Recent provenance studies showed a clear change in sediment provenance at the Paleocene/Eocene transition. Indeed, Thompson et al. (2020) evidence a unimodal age distribution (Hercynian U/Pb age dominant) and old Triassic exhumation ages interpreted as a southern source signature (Ebro massif and Catalanids) for the Paleocene sample while a multimodal U/Pb age distribution and rejuvenated Pyrenean exhumation ages were obtained for the Eocene formations of the Ager basin. However, Nijman (1998) pointed that paleocurrents are flowing to the North in the Ypresian Corçà Formation, and gradually shift and finally strike parallel northwestward transport directions in the upper part making it difficult to source the sediment routing system in the Pyrenees for this period. It seems needed to correlate and compare the Paleocene-Eocene deposits from the eastern Pyrenees (Pedraforca and Ripoll sub-basins) with the Ager sub-basin to decipher if a Pyrenean source is possible or must be excluded for the Ypresian deposits of the Ager sub-basin.

Here we contribute with a magnetostratigraphy-based chronostratigraphy of the Ager Basin. Our new age model provides constraints to clear up the correlation between the eastern and central sectors of the South-Pyrenean foreland. We further calculate the evolution of the subsidence for each sub-basin and discuss the implications and drivers of these changes. We conclude with a novel Early Eocene paleogeographic scenario, where the evolution of the South Pyrenean Zone is refined based on the reconstructed sediment routing systems.

2. Geological setting

2.1. The central Pyrenees

The Pyrenean range is an East-West asymmetrical double wedge orogenic belt resulting from the north directed convergence and collision between the Iberian and Eurasian plates (Choukroune, 1989; Muñoz, 1992; Vergés et al., 2002). Cross-sections based on seismic data (ECORS profile) show evidence of the northwards subduction of Iberia (Muñoz (1992); Teixell et al., 2016). Plate collision lasted from the Late Santonian (Late Cretaceous) until the Oligocene-Early Miocene (Vergés et al., 1995). The southern thrust system developed on top of the subducting Iberian plate, while the northern thrust system formed on top of the European plate (Muñoz, 1992, Vergés et al., 1995; Beaumont et al., 2000). A minimum total shortening of 111 km has been estimated for the Eastern Pyrenees (Grool et al., 2018) which for the central part of the orogen rises to a minimum shortening of 147 km (Muñoz (1992)), whereas a reduced shortening of 75–80 km was proposed by Teixell, 1998) for the western Pyrenees.

The Pyrenees can be divided into five tectonic provinces from South to North: 1) The pro-wedge foreland basin called the Ebro basin evolved bounded by the Pyrenees frontal thrust, the Catalan Coastal ranges (CCR) and Iberian ranges (Fig. 1); 2) The South Pyrenean Zone (SPZ) is a fold and thrust belt that developed from late Santonian to the Oligocene in a piggyback sequence over a Triassic salt decollement (Muñoz et al., 2018; Vergés et al., 2002). 3) The Axial zone is a complex South-verging thrust structure mainly made of Hercynian basement rocks arranged in

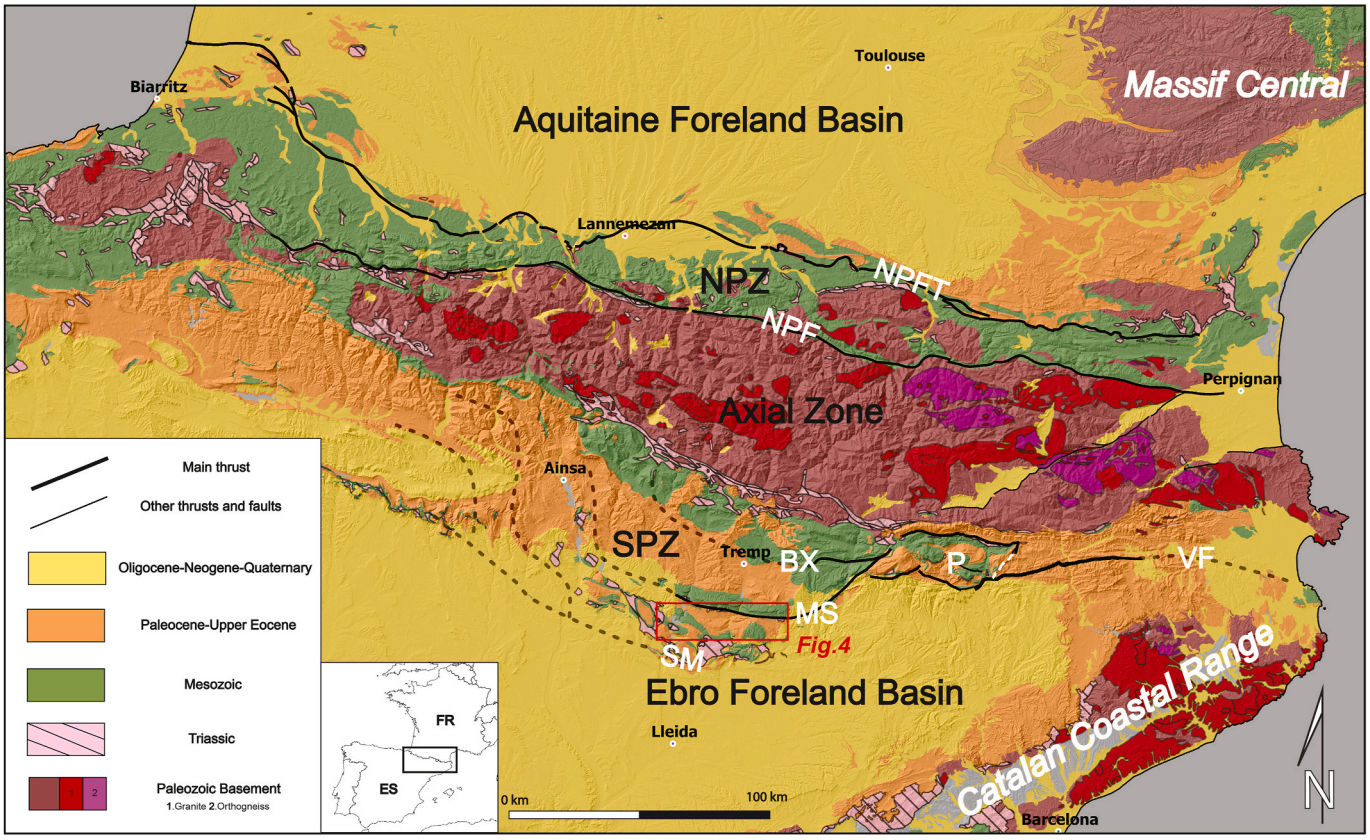

Fig. 1. A Geological map of the Pyrenees and adjacent areas, showing the main structural zones. Red square represents the position of Fig. 4. **NPFT**: North Pyrenean Frontal Thrust; **NPF**: North Pyrenean Fault; **B**: Bóixols thrust; **MS**: Montsec thrust; **SM**: Serres Marginales thrust; **P**: Pedraforca unit. **SPZ**: South Pyrenean Zone, **NPZ**: North Pyrenean Zone. Information extracted from IGME and BRGM shapefiles at 1:1 000 000 and 1: 250 000 scale.

an antiformal stack connected to the SPZ thrusts (Choukroune, 1989; Muñoz, 1992). 4) The North Pyrenean Zone (NPZ) is a narrow retro wedge fold and thrust belt that involves pre-Alpine Paleozoic massifs and inverted Mesozoic pre-orogenic rift related stratigraphic successions (Souquet, 1988). 5) The Aquitaine foreland basin corresponds to the undeformed retro wedge foreland basin located North of the Pyrenees and bounded by the Massif Central at the North-East.

The central part of the SPZ has endured three different episodes of shortening related to the progressive emplacement of the different thrust sheets, from north to south and from older to younger: Bóixols, Montsec and Serres Marginals thrust sheets (Fig. 2). (Muñoz et al., 2018). The prolongation of these thrust sheets towards the Eastern Pyrenees are not straightforward. The Pedraforca unit (Vergés, 1993) is composed of three main sub-units: Upper, Middle and Lower Pedraforca which are interpreted as equivalent to the Bóixols, the Montsec and the Serres Marginals thrust sheets respectively (Muñoz et al., 2018).

The tectonostratigraphic relationships constrain the age of motion of the SPZ thrust sheets. The Bóixols thrust sheet, which originated from the inversion of the Early-Middle Cretaceous marine basins at the southern margin of the Pyrenean rift system (Mencos et al., 2005), shows that deformation started in the Late Santonian and continued during the Late Cretaceous (Lopez-Mir et al., 2014). Afterward, during the Paleocene to the Early Eocene, the Montsec thrust developed (Puigdefàbregas et al., 1986 and Nijman, 1998) as recorded by continental to shallow marine sediments deposited in its footwall, the Ager basin, and in its hanging wall, the Tremp basin (Chanvry et al., 2018). During Eocene times, these two nonmarine to shallow marine basins grade westwards into the slope succession of the Ainsa basin at the footwall of the Montsec thrust (Muñoz et al., 2018).

Southwards, the Serres Marginals thrust sheet is located between the southern thrust front (SM thrust on Fig. 1) and the Montsec thrust (MS thrust on Fig. 1). The Serres Marginals thrust sheet is characterized by an incomplete and thin Mesozoic-Paleogene succession, progressively reducing thicknesses and number of units southwards (Pocoví.Juan, 1978; Muñoz et al., 2018). Triassic evaporites controlled the internal structure of the Serres Marginals thrust sheet by favoring the development of detachment anticlines and diapirs (Santolaria et al., 2015). The emplacement of this unit occurred from Middle Eocene to Early Oligocene (García-Senz and Zamorano, 1992; Teixell and Muñoz, 2000).

2.2. The Paleogene Àger sub-basin (Serres Marginals thrust sheet)

The Ager sub-basin developed at the northernmost part of the Serres-Marginals thrust-sheet, bounded to the north by the Montsec thrust. The Paleogene sediments of the Ager basin form a 35 km elongated east-west asymmetrical syncline, unconformably overlain by the upper Eocene-Oligocene Collegats conglomerates. The northern limb of the syncline dips approximately 80° to the south while the southern limb dips northward between 25 and 50°. The first signs of deformation date from the Palaeocene (Minelli et al., 2013) and lowermost Eocene (Meigs, 1997). During the Palaeocene and Ypresian, the Ager and the Tremp sub-basins were probably connected (Nijman, 1998) depending on the local activity of the Montsec blind thrust. From Early to Middle Eocene times, it evolved into a piggy-back basin. The Millà (SW) and St. Mamet (SE) anticlines outline an irregular southern basin margin with large transversal depressions (Minelli et al., 2013) evidenced by differential subsidence patterns along E-W transects (Colombo and Cuevas, 1993).

The Ager sub-basin infill consists of a relative conformable succession including Paleocene to Early Eocene strata (Fig. 3) unconformably overlain by upper Eocene to Oligocene conglomerates. The succession, from base to top is divided into the Tremp, Àger and Montanyana Groups (Puigdefabregas et al., 1989). The Tremp Group or Garumnian facies (Fontllonga group according to Colombo and Cuevas, 1993) has been divided into 4 units (Galbrun et al., 1993). The first unit (Maçana Fm in Colombo and Cuevas, 1993) consists of 80m thick lacustrine limestones. A reinterpretation of the magnetostratigraphic data of Galbrun et al. (1993), proposes an Early Maastrichtian age for the Maçana Fm (Fondevilla et al., 2019). Above, the second unit (The Figuerola Fm) encompasses 200m of red beds (Lower red Garumnian of Galbrun et al., 1993). A Late Maastrichtian to Early Danian age (base chron C31n to Base C29n) has been ascribed to the Figuerola Fm (Fondevilla et al., 2019). Above, the third unit of ca. 75m corresponds to the Millà Fm., and is equivalent to the Vallcebre limestone, an extensive lacustrine unit that outcrops eastwards in the Vallcebre basin (Sugrañes., 1970). Its age was interpreted as Danian (C29n, according to Fondevilla et al., 2019) or Selandian according to Vicente et al. (2016). The fourth unit is the Perauba Fm (Colombo and Cuevas, 1993), whose lower part is dominantly made of red beds intercalated with fine-grained sandstones interpreted as a low energy mudflat (Colombo and Cuevas, 1993), while the upper part grades from laminated and nodular evaporites to carbonate facies originally interpreted as lagoonal deposits (Colombo and Cuevas, 1993) and later attributed to shallow marine environments (Rossi, 1997). Above these carbonate transgressive beds, a thin unit of nonmarine fluvial to mudflat sediments associated to the Paleocene-Eocene Thermal Maximim (PETM) (Minelli et al., 2013) were deposited. The age of the Perauba Fm ranges from Danian (chron C29n) to Early Ypresian (base of the Ilerdian marine limestone of the Cadí Fm).

The Eocene succession of the Ager syncline includes the Ager and Montanyana groups (Puigdefabregas et al., 1989). The first unit of the Àger group is the Ypresian Cadí formation (50m) which marks the marine flooding of the foreland basin. The Cadí Fm is mainly made of Alveolina, Orbitolites, and Miliolid grainstones organized in coarsening upwards sequences interpreted as littoral bars (Zamorano, 1993). The Cadí Fm is unconformably overlain by the shallowing Figols Sequence (Mutti et al., 1988), comprising three formations: Baronia, the Passarel·la, and the Ametlla Formations (Fig. 4). The Baronia Formation includes tide-dominated prograding delta and shelf sediments with predominant west-oriented paleocurrents (Mutti et al., 1985), organized

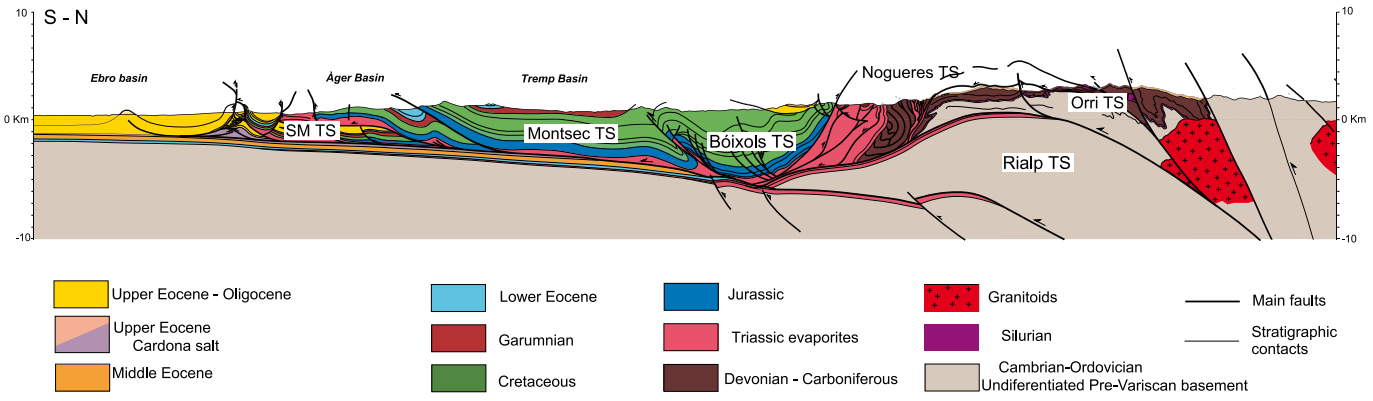

Fig. 2. North-South cross section of the south-central Pyrenees. Modified from Muñoz et al. (2018).

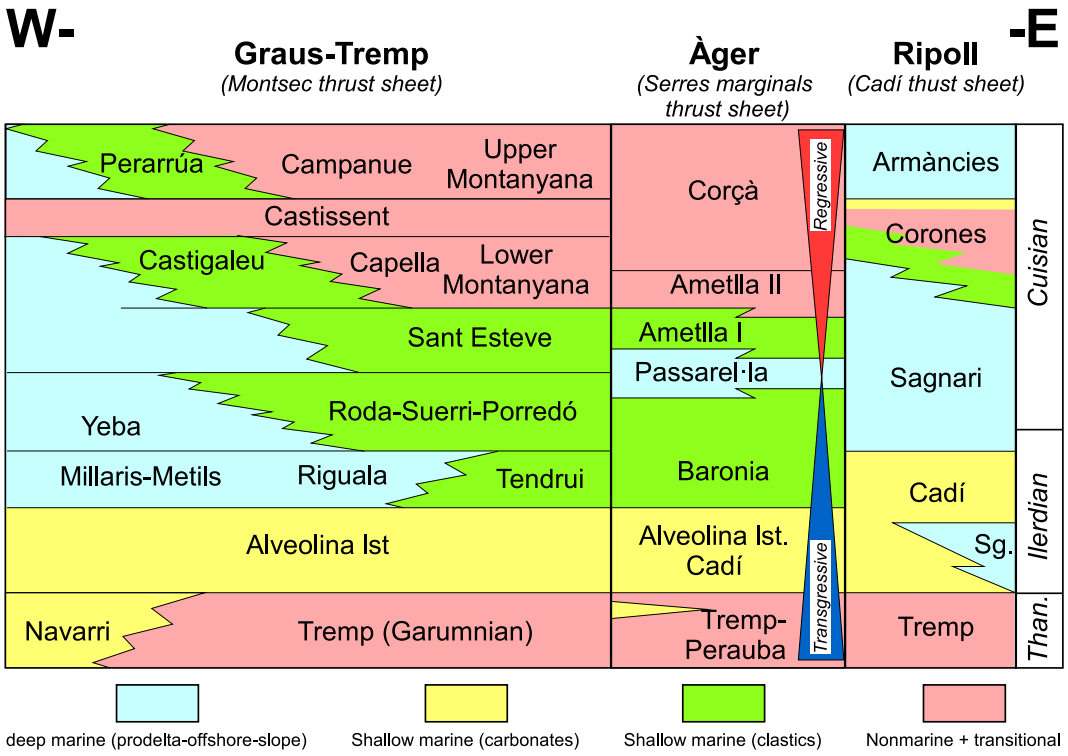

Fig. 3. Stratigraphy of the Ager Ripoll and Graus-Tremp sub-basins including lithostratigraphic subdivision, chronostratigraphic data and depositional setting. Vertical transgressive and regressive trends in Àger basin are represented by blue and red triangles respectively.Tremp -Graus stratigraphy from Garcés et al. (2020). Ripoll stratigraphy from Juvany et al. (2024).

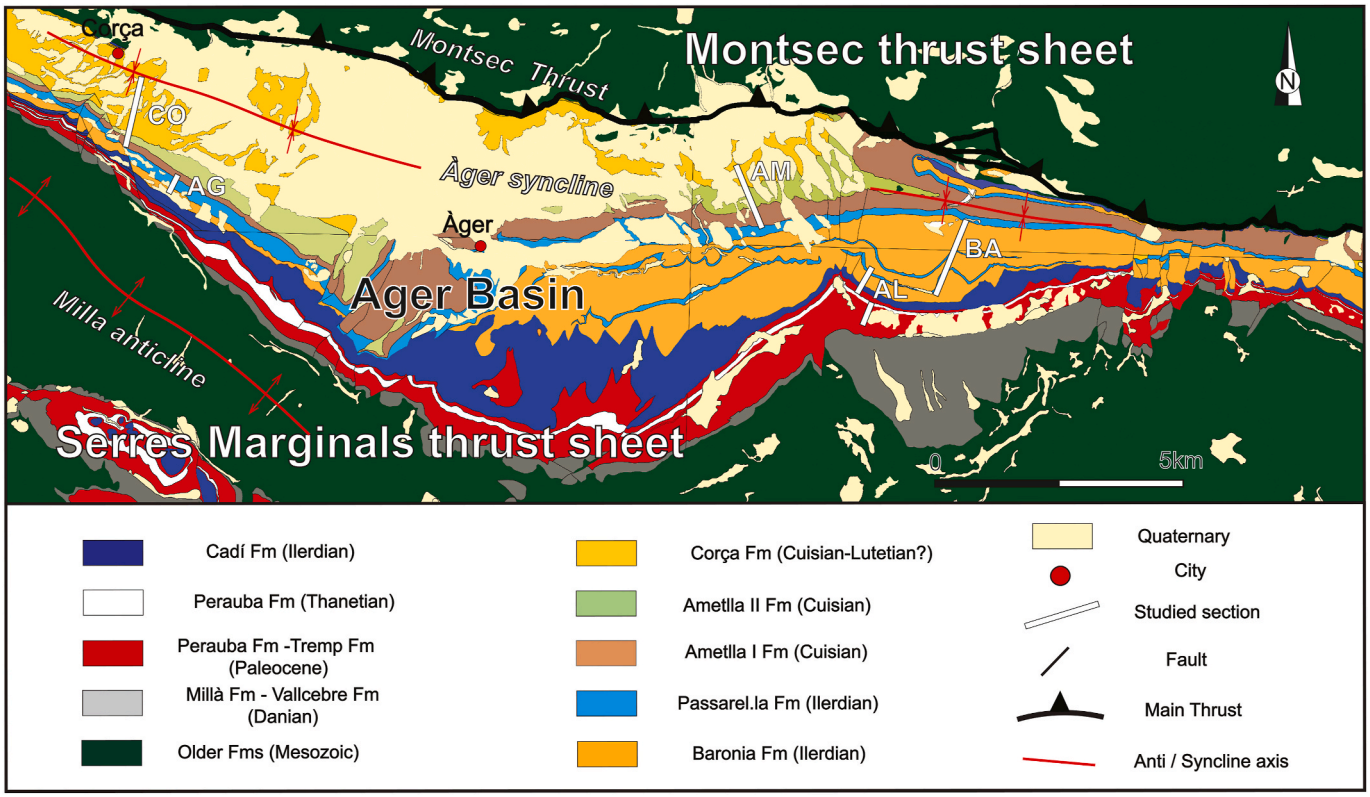

Fig. 4. Geological map of the Ager syncline including the main structural and stratigraphic elements of the area. and the position of the studied sections (White lines). **AL** for Altierres, **BA** for Baronia, **AM** for Ametlla, **AG** for Agulló and **CO** for Corçà. Modified from the Institut Cartogràfic i Geològic de Catalunya (ICGC) 1:25 000 scale shapefiles. EU-DEM Elevation model from The European Environment Agency.

in three sandstones units. The first unit is dominated by bioclastic and sandy tidal bars (stacked compound tidal dunes in Olariu et al., 2012) in a shelf setting, while the second and third units are made of coastal sediments, with estuarine channels, shoals, tidal flats and estuary mouth tidal bars (Mutti et al., 1985). The overlying mudstones of the Passarel·la Formation is an offshore muddy wedge which marks a transgression on top of La Baronia Formation. The lower part contains marine ichnofossils (Chondrites, Zoophycos) indicating a shift towards deeper environments. The upper part shows a restricted diversity of ichnofacies assemblages, suggesting an increase of freshwater input (Olariu et al., 2012). The regressive trend is also marked by the overlying deltaic sandstones of the Ametlla I Formation, developed as a fluvial dominated delta complex with west-oriented paleocurrents (Zamorano, 1993). This unit shows a progradation to the west, within a less confined basin with only subordinate tidal action (Mutti et al., 1985). The overlying white to yellow Ametlla II mudstones represents a finer-grained transitional environment interpreted as lagoonal to lower delta plain environment with low clastic supply (Zamorano, 1993).

The Montanyana group is represented by the Corçà Formation, which unconformably overlies the sediments of the Ager group. The Corçà Fm consists of a succession of silty flood-plain deposits which alternate with at least 10 units of sandstones and conglomerates interpreted as amalgamated fluvial channels. A NW-SE basin axis orientation was proposed by Poyatos-Moré et al. (2013) as confirmed by onlap geometries of the Corçà Fm onto the Ametlla Fm (southern margin) and the Montsec thrust (northern margin). Paleocurrents are directed to the North in the lower part of the formation, and gradually shift to basin-axis parallel northwestward directions (Nijman, 1998). Similarities in facies, lithology and paleocurrent direction of the Corçà Formation with the Castissent Formation (Tremp-Graus basin) led to interpret a connection among them on both sides of the Montsec thrust (Nijman, 1998; Poyatos-Moré et al., 2013).

Biostratigraphic data has been used to establish stratigraphic correlations between the different sectors of the basin. The available biostratigraphy includes fossil assemblages corresponding to several Shallow Benthic Zones (SBZ) and Mammal Paleogene (MP) reference levels. In the Southern flank of the Ager syncline, the Corçà Fm. host the localities of Corçà 0, Corçà 2, Corçà 3, Barranc del Guesot and Masia d'Hereuet (Checa, 2004; Badiola et al., 2009) which include mammal remains in a fine-textured fluvial stratigraphic succession. These findings indicate a lower Eocene age based on their close affinity with faunas of Avenay and Grauves, the reference localities of Mammal Paleogene zones MP 8–9 and MP 10 (Solé et al., 2015).

Earlier studies (Galbrun et al., 1993; Fondevilla et al., 2019) proposed magnetostratigraphic correlations of the Early Cretaceous to Danian sedimentary successions in Ager, but the overlying synorogenic Paleogene sediments have not yet dated with magnetostratigraphy.

2.3. The Paleogene of the pedraforca thrust sheets

The Lower and Middle Pedraforca thrust sheets bear Paleocene and Lower Eocene strata (Fig. 5) (Mató et al., 1994; Vergés et al., 1995; Martínez et al., 2020). The Lower Pedraforca includes sediments of the Tremp Formation overlaid by Ypresian marine deposits of the Cadí--Sagnari formations. The Cadí Formation. consists of platform carbonates, while the Sagnari Fm. consists of offshore marlstones outcropping in a series of disseminated spots (Queralt, Espinalbet, Puig Cubell. The marls of the Sagnari Fm. are better represented in the section of Espinalbet compared to platform carbonates of Cadí Fm. The Early Eocene in the Middle Pedraforca unit is represented by carbonate to mixed platform sediments (Malanyeu), and shallow marine clastic units (Peguera syncline, Fig. 6). Since the shallow marine clastic sediments in the Peguera syncline may represent the lateral equivalents to the shallow marine clastics in the Ager basin, a detailed study of the sedimentology of this succession is developed at the Results section.

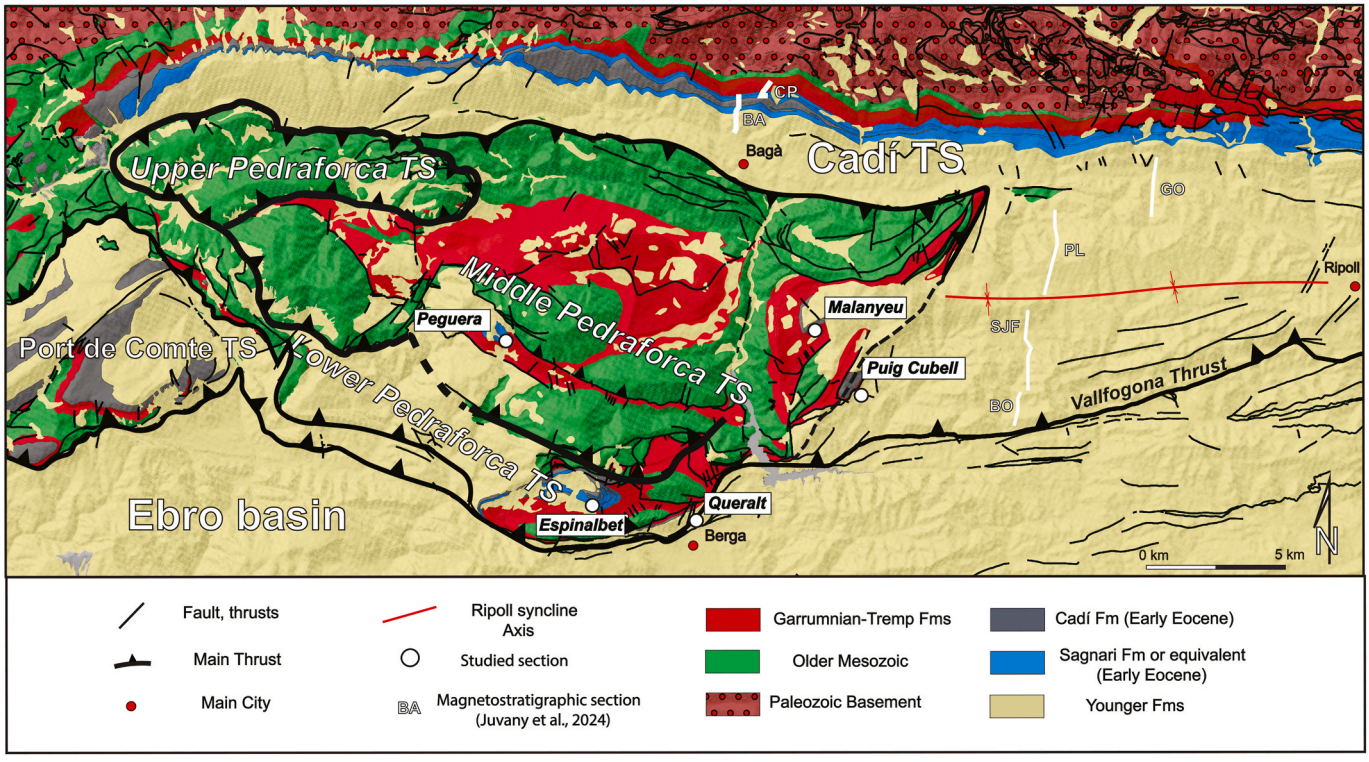

Fig. 5. Geological map of the Pedraforca, Port de Compte and Cadí units. Early-Eocene outcrops in the Pedraforca unit and the Ripoll composite section are highlighted.

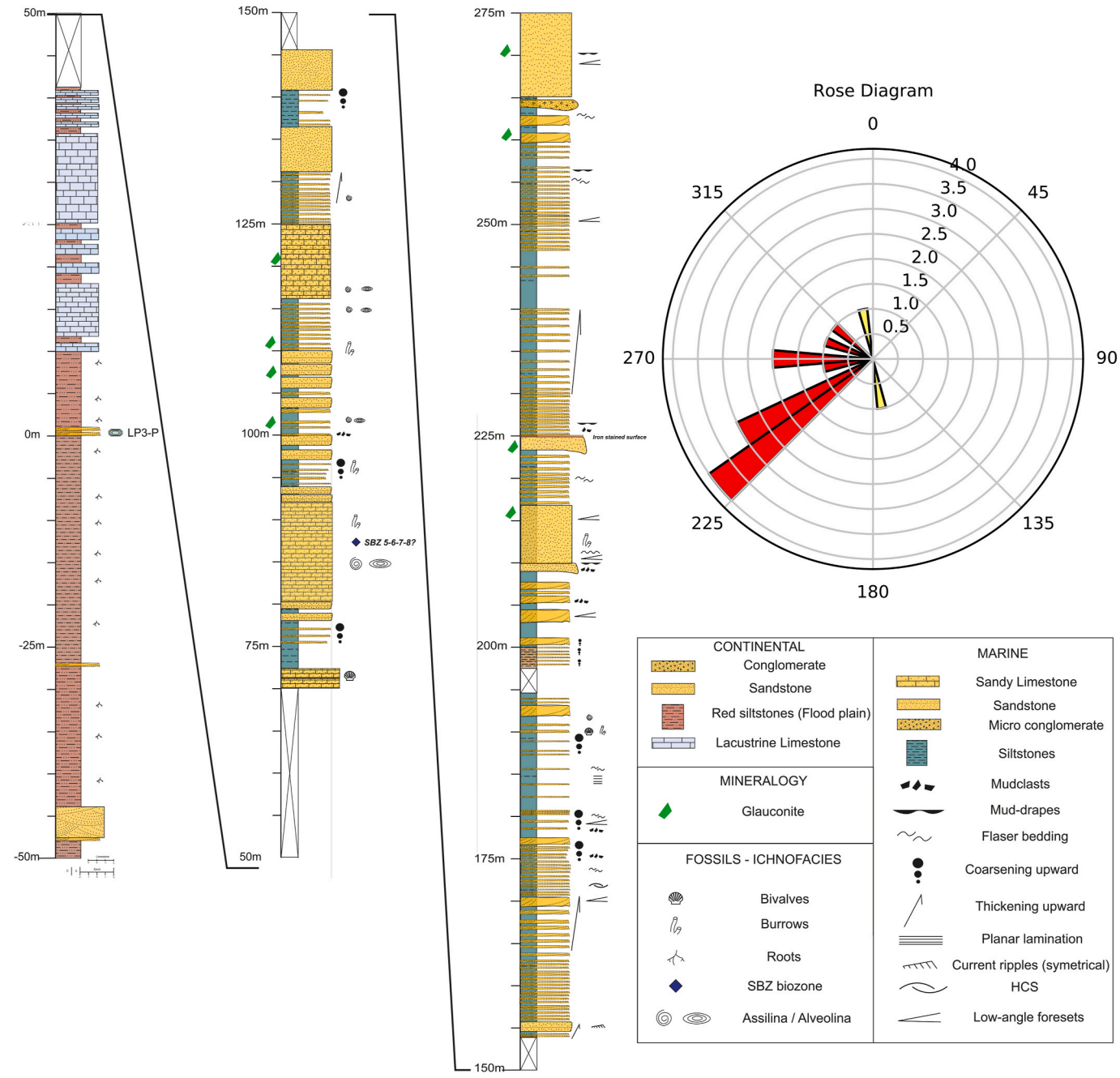

Fig. 6. Stratigraphic log of the Paleocene-Early Eocene sediments of the Peguera section (middle Pedraforca thrust-sheet). Rose diagram shows paleocurrent directions from cross-bedding of the sandstone units (red) and ripple crests alignments (yellow).

3. Methods

3.1. Magnetostratigraphy

Two magnetostratigraphic sections were built on the southern limb of the Ager syncline, one along the Noguera Pallaresa river valley (Eastern section), and the other along the Noguera Ribagorçana valley (Western section). These two sections were divided into sub-sections Alteres (AL), Baronia (BA), Ametlla (AM). Agulló (AG) and Corçà (CO) (Fig. 4). In-situ fresh and fine-grained sediments were targeted to avoid remagnetizations caused by surface alteration. Cylindric drill cores of an average length of 2.0 cm and 2.5 cm wide were extracted using a water-cooled portable electric powered drill and were oriented in situ using a special device made of mounted compass coupled with an inclinometer. Sampling was performed at regular stratigraphic intervals, every 5 m, depending on the availability of required fine-grained sediments (silty and clayey materials). On the eastern part of the Ager syncline, a total of 124 paleomagnetic sites were sampled spanning a total of 1260 m. In the western part, 59 sites were sampled spanning 591m of stratigraphic thickness (see Suppl. Table 1 for sample location + -).

Magnetic measurements were conducted at the laboratory of paleomagnetism housed in the Geo3BCN Institute (CCiTUB-CSIC) in Barcelona. The measurement of the natural remanent magnetization was conducted using a three-axis superconducting rock magnetometer (2G-SRM750). Samples were prepared in the laboratory using a rotary saw to obtain the correct length accepted by the magnetometer (2.1 cm). To isolate the different magnetic components, samples were stepwise thermally demagnetized at 50 °C and after 400 °C at increments of 20 °C.

Magnetic susceptibility was measured at each demagnetization step with a KLY-2 (Geofyzica Brno) to track mineralogical changes when heating.

The Characteristic Remanent Magnetization (ChRM) components were picked after inspection of Zijderveld plots of the samples, and directions calculated using principal component analysis. Low-temperature viscous secondary components were not calculated and excluded from further analysis. ChRM components were ranked according to their quality. Class I refers to ChRM components showing small errors with linear nearly complete demagnetization trends towards the origin of the diagram. Class II refers to ChRM components showing no increasing error and a linear demagnetization trajectory that shows a straight direction towards the origin of the diagram. Class III corresponds to samples showing either irregular demagnetization trends or clustered direction not pointing toward the origin. Class III components were not considered further for magnetostratigraphic correlation.

Pmagpy software (Tauxe et al., 2016) was used to carry out vector analysis. The distribution of ChRM components was analysed in both geographic and tilt-corrected coordinates at site level, and a mean direction of the aggregated Class I and II samples was computed for each sub-section.

The Virtual Geomagnetic Pole (VGP) latitude was calculated for each ChRM direction and plotted against stratigraphic thickness to establish a Local Magnetic Polarity Stratigraphy (LMPS). We attributed positive VGP latitudes to normal polarity, and negative VGP latitudes to reversed polarity. Only stratigraphic intervals having two or more consecutive samples of the same polarity were defined as polarity magnetozones. Correlation of the LMPS with the Geomagnetic Polarity Time Scale (GPTS, 2020; Gradstein and Ogg, 2020) was carried out after the integration of previous magnetostratigraphic data and existing and newly acquired marine and continental biostratigraphic data located in our own new stratigraphic logs.

3.2. Subsidence analysis

Subsidence analysis was carried out on the composite succession (1599 m) assuming a local isostasy model. The numerical age of formation boundaries was derived from interpolation of calibrated magnetostratigraphic boundaries. Formations and magnetostratigraphic boundaries combined were used to divide the succession into units of known age and relatively homogeneous lithology and bathymetry. Decompacted thickness calculation was based on Van Hinte (1978) for changes in porosity with depth. Initial porosity and depth-porosity constant c were based on Sclater and Christie (1980) values for terrigenous and carbonate sediments. Paleobathymetric values were taken from Vergés et al. (1998), and applied by correspondance of depositional environment to the Ager formations. Sea-level from Miller et al. (2020) was used. We did not consider the errors associated with porosity and depth-porosity constant c. Tectonic subsidence was calculated by means of back-stripping techniques based (Steckler and Watts, 1978). Our calculations assumed a density of 3.3 g cm^{-3} for the asthenosphere and 1 g cm^{-3} for water.

4. Results

4.1. ChRM characteristics and age of magnetization

A total number of 183 samples were processed in the laboratory and succeeded stepwise thermal demagnetization until complete removal of the NRM (Supplementary material). All the samples showed a low-temperature viscous component that is removed between 200 °C and 300 °C (Suppl. Fig. 1). This component is generally directed toward the North-East or to the North, mostly representing a viscous component. ChRM components with dual polarity were often revealed at temperatures above 250°-300 °C, and maximum unblocking temperatures that were dependent on the lithology. Tremp and Corçà Fm red beds yielded unblocking temperatures around 660 °C, suggesting hematite as the principal magnetic carrier. Differently, lagoonal and platform carbonates interbedded in the facies of AL, AM and AG yielded unblocking temperatures between 300 and 440 °C, which points towards magnetite as the magnetic carrier. Marlstone from the deltaic Baronia and Passarel·la fm. yielded unblocking temperatures below 500 °C also suggesting magnetite as the principal magnetic carrier. ChRM directions were classified in 32.6% of Class I, 55.1% of Class II and 12.3% of Class III. The mean ChRM direction of each section was calculated from the set of samples of Class I and II, in both geographic and tectonic corrected coordinates (Fig. 7, Suppl. Figs. 2 and 3). The summary results of the Eastern and Western sections show that mean directions yielded northerly declinations with positive inclinations, between 44° and 47°, after correction for bedding tilt, which is coherent with the expected field for the site latitude (Table 1). This observation, together with occurrence of several reversals along the study stratigraphic interval, suggests that the remanence acquisition predates tilting of beds. A classic fold test could not be carried out because all the sections are on the same southern limb of the Ager syncline (Fig. 4), and there is no significant variations in bedding attitude between sections.

4.2. Local magnetostratigraphy

4.2.1. Eastern Ager section

The Alteres (AL) subsection constitutes the base of the Eastern section of the Ager Basin, it is located in the Baronia, to the east of the C-13 road. The AL section starts just above the Millà Fm., at the base of the Perauba Fm. The average bedding dip of the sampled interval is 354°/12° (dip direction/dip). The magnetic polarity of the AL section is predominantly reverse, with one normal magnetozone (N1 in Fig. 8). Additionally, a few single sample normal polarity intervals were observed within the Perauba Fm. We consider these features not reliable for correlation purposes, as they may represent short reversals not represented in the GPTS.

The base of the Baronia (BA) section is 500m eastwards of the AL section, along the C-13 roadcut and continues upwards in the barranc de Montnar stream. This section spans the Upper part of the Perauba Fm including the PETM and the Cadí, Baronia and Passarel·la formations. The average bedding dip of the sampled interval is 010°/28°. One reversed (R2) and one normal (N2) magnetozone have been identified in this section (Fig. 8). The mean normal and reverse polarity directions yield quasi-antipodal vectors and north-directed (Suppl Fig. 2).

The Ametlla (AM) subsection starts west of the Casetes de l'Estació along the road C-12 and continues northwards towards the Serrat de Pujol. It spans the Ametlla I and II and the lower part of the Corçà Fm. Correlation of the BA and AM section was feasible following the distinct expression of the Passarella-Ametlla Formation boundary across the region. Three normal (N2 to N4) and two reversed (R2, R3) magnetozones have been identified (Fig. 8). Like in the BA section, mean normal and reverse polarity directions yielded antipodal directions (Suppl Fig. 2).

4.2.2. Western Ager section

The Agulló (AG) subsection starts in the barranc de Contorna up to la Tosseta locality along the road between Millà and Agulló. This section starts just above the upper part of the Baronia Fm. and spans the entire Passarella, Ametlla I and II in the western part of the sub-basin. The average bedding dip of the sampled interval is 000°/28°. One reverse and one normal magnetozone have been identified in the AG section (Fig. 8) and mean normal and reverse polarity directions succeeded in yielding antipodal directions (Suppl Fig. 3).

The Corçà (CO) subsection is located 2 km west of AG subsection, with its base near the Masia de l'Hereuet. It extends the record in the upper Corçà Fm. toward the town of the same name. The base of the CO section can be easily correlated with the top of the AG section following a carbonate rich level that forms an east-west relief in the topography.

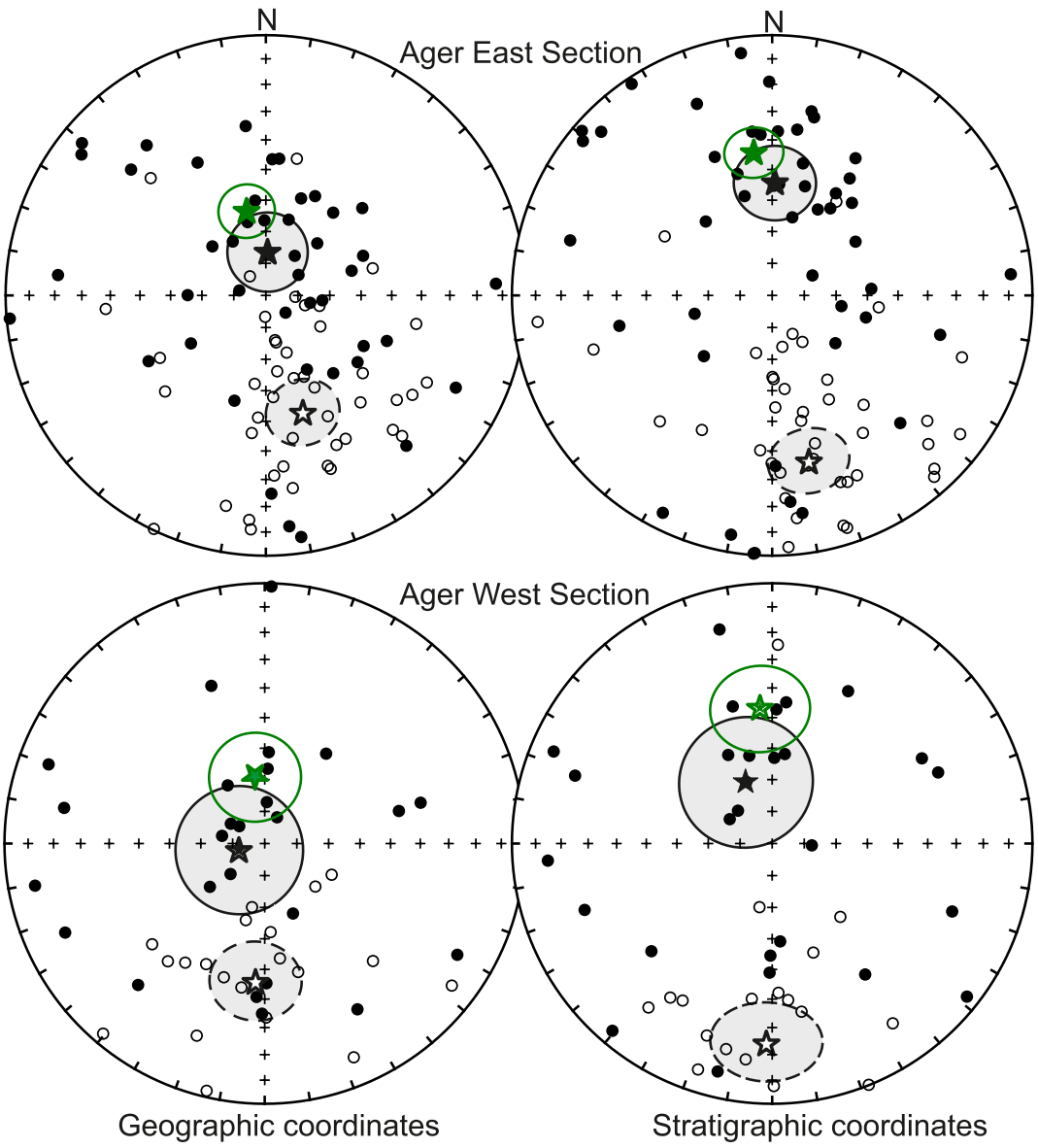

Fig. 7. Stereonet projection of ChRM directions of the Eastern and Western sections of the Ager basin. Black stars: The mean and fisher statistics of both normal and reversed polarity directions. Green star: Overall mean after flipped all to normal. Fisher statistic parameters listed in Table I.

Table 1
Mean paleomagnetic directions of the Eastern and Western Ager sections and associated fisher statistics. N: Normal polarity; R: Reverse polarity; R→N: All flipped to Normal polarity.

	Pol	N	geographic coordinates				stratigraphic coordinates			
			Dg	Ig	k	a95	Ds	Is	k	a95
Ager West	N	25	255	82	7	13	337	69	3	21
	R	21	184	−46	3	20	182	−24	6	15
	R– > N	**46**	**352**	**69**	**3**	**14**	**355**	**47**	**3**	**15**
Ager East	N	40	002	76	4	13	001	54	4	12
	R	49	163	−51	5	11	168	−35	4	11
	R– > N	**89**	**347**	**63**	**4**	**9**	**353**	**44**	**4**	**9**

The average bedding dip of the sampled interval is 020°/15°. 2 normal (N4, N5) and 2 reverse (R4, R5) magnetozones have been identified in the CO section (Fig. 8). The mean normal and reverse polarity directions fail to yield antipodal directions (Suppl Fig. 3). This error may result from the combination of an inclination error that preferentially affects the reversely magnetized red beds from the Corçà Fm, and the contribution of a recent normal polarity partial overprint.

4.3. Sedimentology of the Peguera syncline lower Eocene clastic units

The Paleogene units cropping out at the core of the Peguera syncline consist first of a lower red-bed unit (Tremp Fm, up to 400m) capped by lacustrine limestones interpreted as upper Palaeocene as they overlay the reptiles Sandstone (Late Maastrichtian) and the Vallcebre limestone (Danian) (Oms et al., 2007). These strata are overlaid by Early Eocene

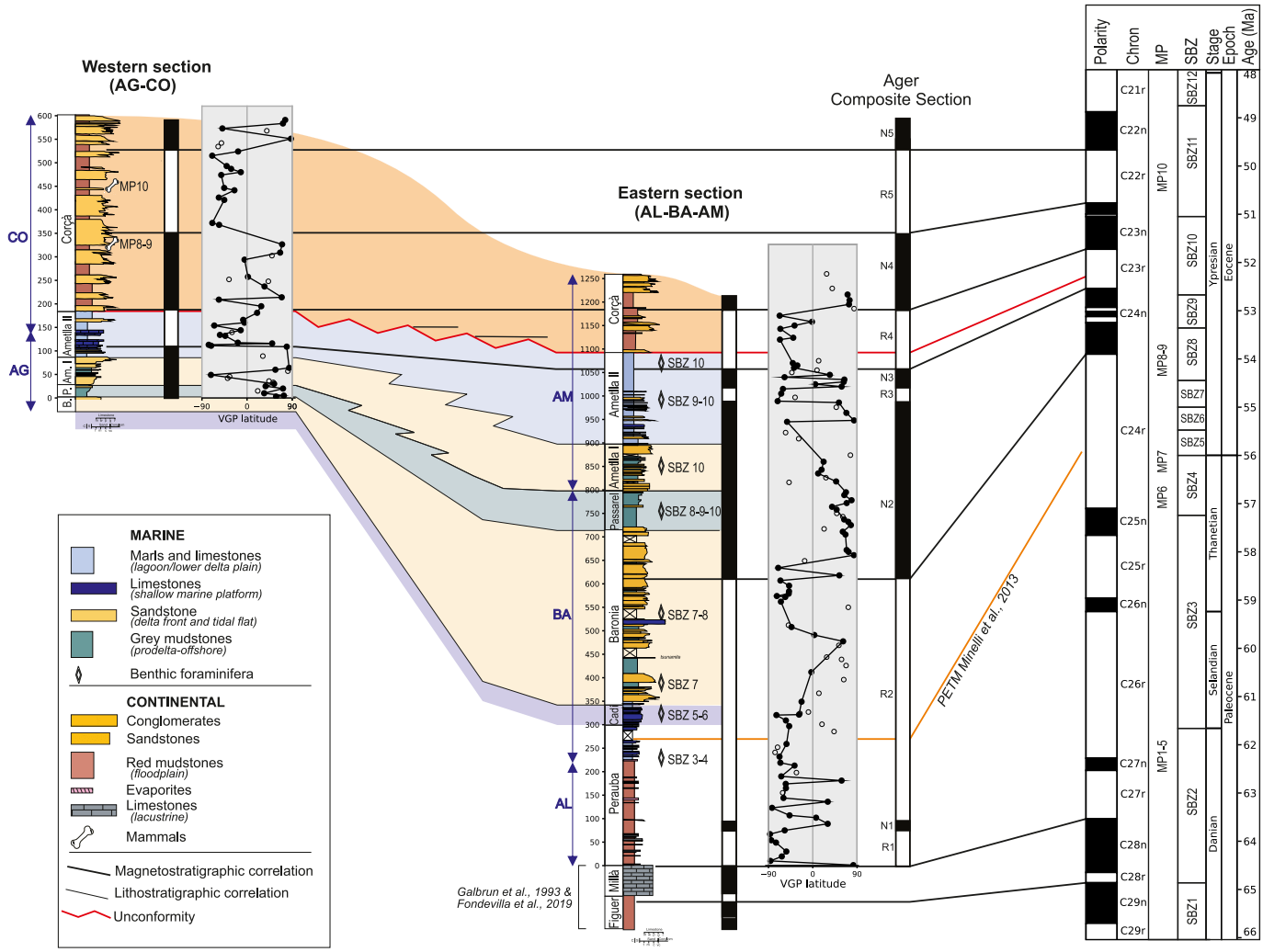

Fig. 8. Composite Local Magnetic Polarity Stratigraphy (LMPS) of the Ager syncline built from the correlation of the AL (Altierres), BA (Baronia), AM (Ametlla), AG (Agulló) and CO (Corçà) sections. Magnetostratigraphy of the Figuerola and Millà formations after Galbrun et al. (1993) and Fondevilla et al. (2019). Right: Correlation of the LMPS with the Geomagnetic Polarity Time Scale (GPTS, Gradstein and Ogg, 2020). MP: Mammal Paleogene Reference levels; SBZ: Shallow Benthic Zones from Serra-Kiel et al. (1998, 2020). Notice the thickness reduction of Baronia, Passarel·la and Ametlla formations from E to W due to differential subsidence related to Milla anticline Growth.

sediments with a preserved thickness of approximately 200m (Fig. 6). The Eocene succession consists of marine sediments representing mixed platform to deltaic environments. Calcarenites appear to be dominant at the base of the section, while the clastic content increases upwards. Sandstones are fine to very coarse, poorly sorted, and with abundant bioturbation. Coarsening and thickening up sets are common, typically with mud-drapes, and often showing flaser bedding, and mud-clasts. Erosive bases, planar lamination, symmetrical ripples, hummocky cross stratification, large-scale foresets, low angle foresets and channels can be observed. The orientation of crossbedding indicates average westward directed paleocurrents, and ripple crest alignment suggests a local coastline with an NW -SE orientation (Fig. 6). Bivalves (Oysters), Echinoids, Bryozoan, and benthic larger foraminifera such as Assilina and Alveolinids are abundant. Glauconite content increases up section.

The intense interdigitation between clastic dominated and carbonate-bioclastic rich facies suggests the coalescence of carbonate platforms and siliciclastic systems in Eocene times in the Peguera. These deposits are tide-influenced as evidenced by mud-drapes and flaser bedding but also influenced by fair weather and storm waves. The overall depositional setting is interpreted as a sandy, relatively high energy SW facing siliclastic shoreface oriented approximately NW-SE. Periods of embayment (tidal influence) alternate with periods of higher energy and clastic input through channels in an open sea (wave influence). The detailed age is uncertain but can be attributed to the Early Eocene as this formation directly overlies the Paleocene Tremp Fm.

5. Discussion

5.1. A magnetostratigraphic framework of the Ager basin

5.1.1. Local Composite Magnetostratigraphy

A Local Composite Magnetostratigraphy (LCM) of the Ager syncline succession was built by integrating the data provided here with earlier works (Galbrun et al., 1993; Fondevilla et al., 2019).

Along the eastern part of the Ager syncline, AL, BA, and AM subsections combined provide a complete record of the Paleogene stratigraphy, encompassing the Tremp-Perauba Fm. to the lower part of the Corçà Fm. The substantial overlap between the subsections ensures the completeness of the resulting LCM. The AL section shows two reverse magnetozone (R1 and R2) and one short normal magnetozone (N1). The magnetozone R2 is traced to the BA section. Above, a normal magnetozone (N2) extends throughout the upper Baronia Fm. and the whole Passarel·la Fm. The correlation between BA and the AM sections is based

on the distinct expression of the Passarella-Ametlla Fm. boundary across the region. Accordingly, the top normal magnetozone in BA is interpreted as the lower normal magnetozone in AM section (N2 in Fig. 8). The AM section continues with the short magnetozones R3, N3 followed by the larger R4 and N4 magnetozones.

The western subsections (AG and CO) allowed us to extend the record upwards into the Corçà Fm. Correlation between the AG and CO section relies upon the Ametlla II-Corçà Formations boundary, which is marked by a distinct limestone level. In the AG-CO composite section, three normal and two reverse magnetozones were identified.

Correlation between eastern and western margins of the Ager syncline was feasible following the cartography of the Passarella Fm., which represents a rapid transgressive phase across the basin. Therefore, we consider that the normal magnetozone observed in the Passarella Fm. in both the eastern and western sections indeed represent the same magnetozone N2 of the composite section. Thickness variations between both sections could be a combination of differential subsidence due to tectonics in a wedge top setting. Above, the reversed magnetozone observed in the Ametlla Fm. in both the eastern and western sections would correspond to R4. The short magnetozones R3 and N3 found in the east are not recorded on the western side of the syncline and might represent short sub-chrons. The upper part of the CO section depicts the R4, N4, R5 and N5 magnetozones, which do not have their equivalent in the eastern sections sector due to erosion. The correlation of all the eastern and western sections results in a 1599m thick LCM of the Ager syncline which includes 5 reversed and 5 normal magnetozones. It is worth noting that the positive cross-correlation of magnetozones and lithostratigraphic boundaries between East and West is indicative of the primary character of the ChRM.

5.1.2. Biostratigraphic constraints

A first-order chronostratigraphic scheme of the Ager basin infill is available from the well stablished lithostratigraphic subdivision and the biostratigraphic constraints provided preferentially from marine strata. A compilation of biostratigraphic data, and their Shallow Benthic Zone attribution (Serra-Kiel et al., 1998) is shown in Table 2. This table is based on original data from Llompart (1977), Luterbacher (1969, 1973), Ferrer et al. (1973) and Crusafont et al. (1968) later assigned to the lithostratigraphic units (Zamorano, 1993; García et al., 2017) and combined with more recent data (Teixell and Leyva, 2006; Saula et al., 2017). According to the benthic foraminifera, the age range of the succession spans from Thanetian (SBZ 3 and 4) in Perauba Fm. to early Cuisian (SBZ 10) in Ametlla Fm. From this compilation we conclude that the benthic foraminifera biostratigraphy is a first order constraint for the magnetostratigraphic correlation of the Ager LCM with the Geomagnetic Polarity Time Scale (GPTS, Gradstein and Ogg, 2020). With regards to continental chronology, mammal sites in Corçà Fm. (Checa, 2004; Badiola et al., 2009) include faunas assigned to MP 8–9 (Corçà 0) and MP 10 (Corçà 2 and 3) that are thought to correlate with the Cuisian stage, within Ypresian (Speijer et al., 2020).

5.1.3. Correlation with the GPTS

A correlation with the GPTS can be confidently assessed on the basis of the above biostratigraphic constraints. The eastern Ager section starts on top of the Millà Fm, which was dated as Early Danian (chron C28n) (Galbrun et al., 1993; Fondevilla et al., 2019). The normal polarity sample observed at the base of the AL section is interpreted as the uppermost part of chron C28n found in the underlying Millà Fm. Subsequently, we correlate magnetozones R1 and R2 with chrons C27r, C25r and C24r including faunas ranging from SBZ3 to SBZ8. The two isolated normal samples observed in the Perauba Fm. might represent either chrons C27n, C26n and C25n but they are only represented by a single sample. We interpret the poor record of these relatively short normal chrons as a result of delayed magnetization during a period of dominant reversed polarity in a context of very low sedimentation rates. For this to happen, the magnetization lock-in depth should be greater than the thickness of the missing magnetozones. As a result, the correlation of magnetozone N1 with either C27n, C26n or C25n remains unsolved.

Table 2
Synthesis of the Biostratigraphic data (benthic foraminifera and mammals) from the Àger basin. Lithostratigraphic formations are assigned a biochronological age according to occurring fossil taxa. SBZ: Shallow Benthic zones. MP: Mammal Paleogene reference levels.

		Alveolina (Glomalveolina) primaeva	*A. levis*	*A. ellipsoidalis*	*Alveolina globula*	*A. Avellana aurignacencis*	*A. Varians*	*A. dolioformis*	*A. (Glomalveolina) pasticillata*	*A. (Glomalveolina) lepidula*	*A. Moussolensis*	*A. subpyrenaica*	*A. Aragonensis*	*A. corbarica*	*A. ilerdensis*	*A. canavarii*	*A. trempina*	*A. Schwageri*	*A. oblonga*	*Diacodexis corsaensis nov. sp.*	*Diacodexis sp.*	
Cuisian	MP 10																				■	
Cuisian	MP 8+9																			■		
Middle Cuisian	SBZ11																		■			
early Cuisian	SBZ10														■	■		■	■			
late Ilerdian	SBZ9									■			■		■		■					
Middle Ilerdian 2	SBZ8									■			■	■	■							
Middle Ilerdian 1	SBZ7									■	■	■	■									
early Ilerdian 2	SBZ6							■	■	■												
early Ilerdian 1	SBZ5			■	■	■	■	■		■												
late Thanetian	SBZ4		■																			
early Thanetian	SBZ3	■																				
Cuisian	Corçà fm.																					MP 8+9-10
early - Middle Cuisian	Ametlla II Fm																■		■			SBZ9-11
early - Middle Cuisian	Ametlla I Fm																	■	■			SBZ10
Midle Ilerdian 2 /early Cuisian	Pasarela Fm													■	■	■	■					SBZ8-10
Middle Ilerdian 1	Baronia Fm									■	■	■	■	■								SBZ 7-8
early Ilerdian 1 & 2	Cadí Fm			■	■	■	■	■	■	■												SBZ5-6
early Thanetian/late Thanetian	Perauba Fm	■	■																			SBZ3-4

The normal magnetozone N2 observed from the upper part of the Baronia up to the Passarella and Ametlla I formations is interpreted as chron C24n as it coincides with the occurrence of SBZs 8–9 and 10 in the Passarella and Ametlla Formations respectively. R3, recorded in the eastern section, is correlated with one of the short reversed C24n subchrons (C24n.1r or C24n.2r). Nevertheless, R3 is not recorded in the western section, probably because of the lack of suitable lithologies due to the abundance of sandstone and sandy silts, combined with low sedimentation rates.

The magnetozone R4 is correlated with chron C23r and coincides with the occurrence of SBZ10 in the Ametla II Fm. Magnetozones N4, R5 and N5 are correlated with chron C23n, C22r and C22n respectively. The mammal localities yielding an Ypresian age (MP8-9 and MP10 levels) for the deposits of the Corçà Fm. agree well with this correlation.

5.2. Sediment routing systems and Paleogeography

5.2.1. Stratigraphic cycles

The Danian-Late Cuisian succession of the Ager syncline can be divided into one major transgressive-regressive cycle. The transgressive part starts with the lower part of the Perauba Fm, interpreted as fluvial floodplains (Colombo and Cuevas, 1993) grading from laminated and nodular facies of evaporitic deposition to carbonate facies and bioclastic complex in the upper part and interpreted as lagoonal deposits (Colombo and Cuevas, 1993). The transgressive trend continues in the carbonate platforms of the Cadí Fm. and is restrained by the progradation of the tide-influenced delta of the Baronia Fm. before reaching the Passarel·la Fm. interpreted here as the maximum flooding surface as it marks the start of a general regressive trend. The regressive part of the cycle continues in the freshwater influenced delta of the Ametlla I Fm. grading into the marginal and restrained coastal deposits of the Ametlla II Fm. and the non-marine Corçà Fm. These deposits involve shallow marine, transitional paleoenvironments, which are prone to respond to higher frequency oscillations. Several transgressive and regressive trends are observed in the Perauba, Baronia and Ametlla I-II which probably resulted from cyclicity of higher order. Other significant horizons punctuate these trends, such as the marine wedge in the uppermost Palaeocene (Tremp Fm.) corresponding to the "Th-1" and/or "Th-2" Thanetian marine pulses identified in the Tremp basin (Tremblin et al. (2022), the abrupt influx of coarse-grained siliciclastics at the Paleocene-Eocene boundary (Minelli et al., 2013), the switch from carbonate platform to siliciclastics (Cadí-Baronia transition), and the flooding event within the Ametlla II unit represented by shallow marine carbonates.

5.2.2. Correlation between sub-basins

After structural restoration to Palaeocene-Ypresian stage, the Peguera syncline, on the hangingwall of the Middle Pedraforca-Montsec Thrust, would correspond to a wedge top depozone equivalent to the Tremp-Graus sub-basin. The Ager sub-basin, located on the footwall of the Montsec Thrust, would have been the foredeep, likewise the Espinalbet section further East (footwall and close to the Middle Pedraforca Thrust). Cadí and Port de Comte units, also in the footwall but farther south would correspond to a more distal forebulge position whereas Queralt outcrops would be in an intermediate position between the foredeep and the forebulge depozones on the Lower Pedraforca Thrust Sheet (Fig. 9).

In the Cadí thrust sheet (Ripoll syncline), the Thanetian-Middle Cuisian deposits show one transgressive-regressive cycle in a forebulge setting (Juvany et al., 2024). The transgressive part includes red alluvial facies (Tremp Fm.) that evolve into lacustrine (Van Eeckhout et al., 1991), and then the marine strata of Cadí and Sagnari formations. The regressive trend is evidenced by the lower Corones Fm. that culminates in non-marine red beds. An overall synchronous similar trend occurs in other south-Pyrenean areas such as Port de Comte, Tremp-Graus and Ager basins. The transgressive deposits in Ager, formed by the Perauba-Cadí-Baronia-Passarella formations, followed by the regressive succession of Ametlla I, Ametlla II and Corçà are time-equivalent to the transgressive-regressive cycle in the Ripoll syncline (Fig. 10). The maximum regression culminating this cycle was coeval with a global sea-level fall (Miller et al., 2005), but a tectonic uplift (Puigdefàbregas et al., 1986; Marzo et al., 1988), a pulse of exhumation in the hinterland at 50Ma (Whitchurch et al., 2011), and a combination of all factors (Castelltort et al., 2017) have been considered to play a role. Whatever the dominant forcing factor, this situation favoured an increase in the supply/accommodation ratio, sediment bypass and the advance of the clastic systems.

In the Ripoll syncline, a renewed transgression (Fig. 10) started at the Late Cuisian, during upper chron C22r, in the upper Corones Fm. (Juvany et al., 2024). This transgression is attributed to the local tectonic load of the initial emplacement of the Lower Pedraforca Thrust Sheet (Puigdefàbregas et al., 1986; Vergés et al.,1998), and the consequent forelandwards migration of the lithospheric flexure of the Iberian plate under the overriding European plate. This transgressive event is not recorded or not seen in the Ager syncline since during this period there is continued deposition of the fluvial Corçà Fm. until late Cuisian (C22n). However, this change from regressive to transgressive is also observed in the Graus-Tremp basin (Fig. 10) with the superposition of Perarrúa Fm. shallow marine deposits on top of Castissent Fm. The presence of this transgressive event in a more proximal wedge top location, with higher subsidence and sedimentation rates, points to the loading of the axial zone antiformal stack (Vinyoles et al., 2021).

5.2.3. The Early Eocene sediment routing

As introduced earlier, some authors (Mutti et al., 1985; Dreyer and Fält, 1993; Martinius, 2012) show the Ager and Tremp basins connected westwards to the sea and disconnected towards the eastern margin of the basin. On the other hand, Nijman, 1998, Martinius, 2012; Olariu et al., 2012, suggest an additional marine connection towards the east.

In the Ripoll syncline, a change in the sediment provenance is observed. Composition of the continental Tremp Fm. indicates catchment areas towards the SE, in the Ebro and Montseny massifs, while the overlying marine sediments of the Sagnari Fm. point to a Pyrenean source (Odlum et al., 2019) (Fig. 11a and b). In the Ager syncline, same change in provenance occurs at the transition from continental to marine sedimentation (Tremp to Baronia Fms) (Thomson et al., 2020). At that time, geohistory analysis depicts no major change in the tectonic subsidence both in the Ripoll syncline (Juvany et al., 2024) and in the Ager syncline (Fig. 9), thus indicating that the sediment flux re-organization was unlikely driven exclusively by tectonics. Preceding the shift in sediment provenance, there is a period of development of carbonate platforms (Cadí Fm – Alveolina limestone) along the southern margin, grading northwards into deeper environments (Sagnari Fm.) (Fig. 11b and c). They represent a generalized transgression in the Pyrenean domain that generated a E-W oriented seaway separating a northern Pyrenean domain from a southern (Ebro massif-Catalan Coastal Ranges) domain. This period correlates with a global sea-level rise during C24r Haq et al., 1987, Miller et al., 2005; Miller et al., 2020). As a result, a break in the sediment routing fairway took place, as the flooded regions inhibited the transport of detrital material from the southern and eastern emerged domains to the Pyrenean foredeep. Consequently, the Ilerdian units of the Peguera syncline represent along with La Baronia, Roda and Figols formations the first clastic sedimentary systems of the South-Pyrenean Zone that solely drained the Pyrenean range.

Resulting from the simultaneous emplacement of the Middle Pedraforca-Montsec and possible initial movements of the Serres Marginales-Lower Pedraforca Thrusts or growth of salt pillows, a series of folds may have been generated both in the wedge top and distal foreland depozones. Carbonate production would localize atop of growth structures (submarine anticlines), while clastic sedimentation would be confined along synclines (Martínez et al., 1988). Subaerial

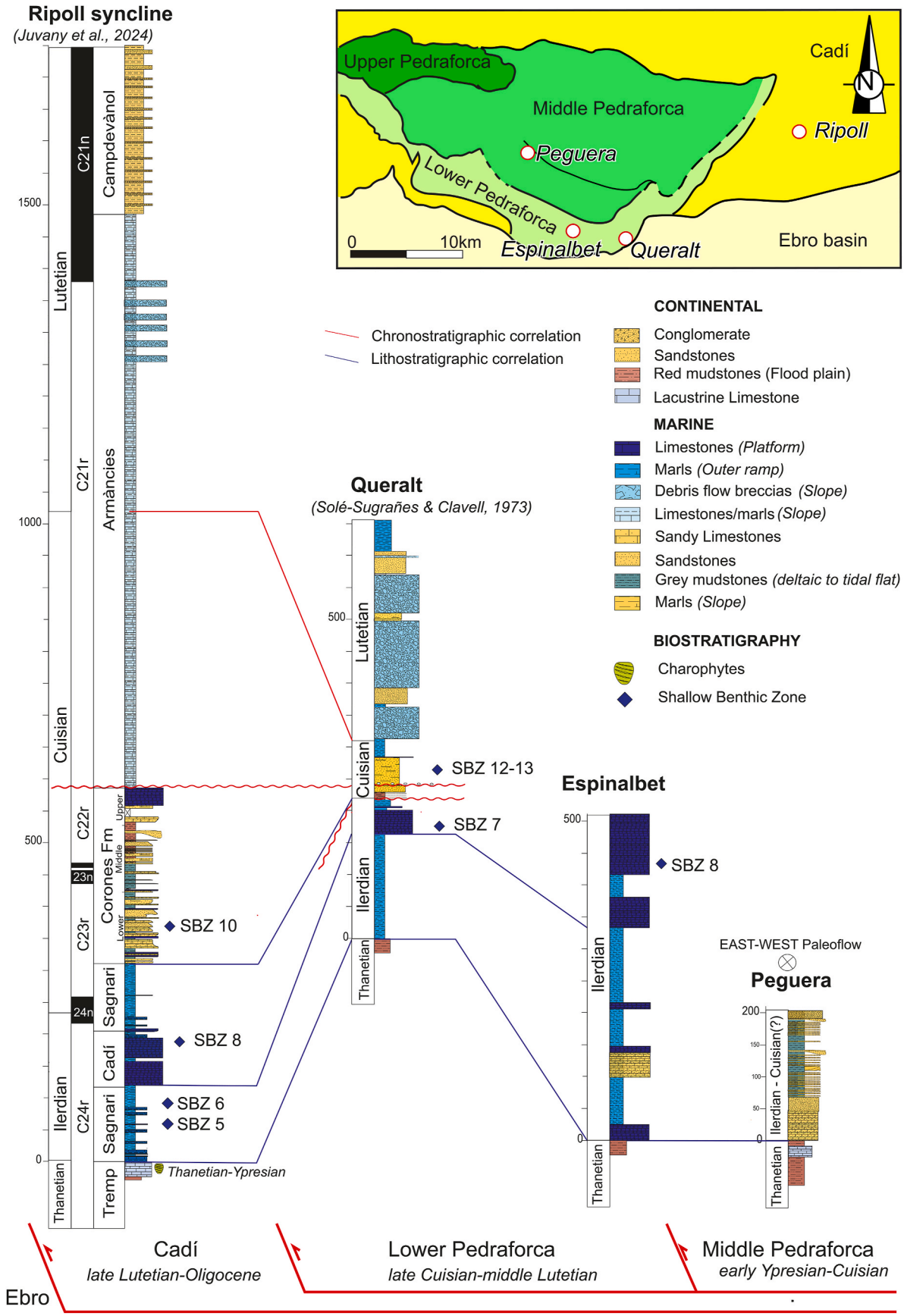

Fig. 9. Correlation of the Ripoll and Pedraforca sub-basins. Queralt stratigraphic column from Solé Sugrañes and Mascareñas, 1970. See Fig. 5 for location. The sketch below shows the location of the sections in relation to the Eastern Pyrenees structural units.

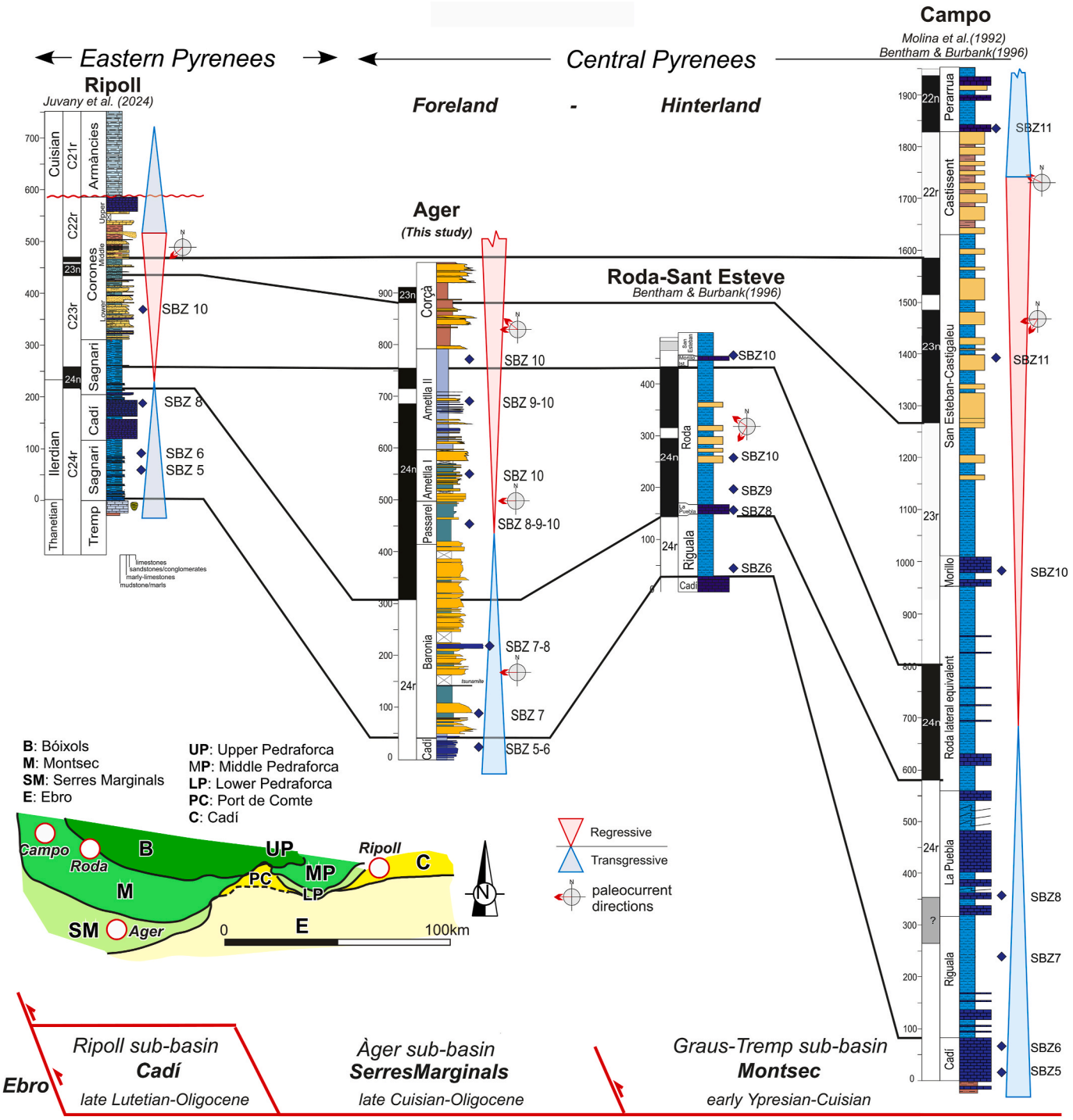

Fig. 10. Correlation of the Ripoll, Ager and Tremp sub-basins. Ripoll section from Juvany et al. (2024); Magnetostratigraphy of the Campo section from Bentham and Burbank (1996), benthic foraminifera from Tosquella (1988, 1995), Samsó (1988) and Molina et al. (1992). Inset map represents the present-day location of the sections. The sketch below shows their relation to the main south-pyrenean structural units.

anticline growth, acting as topographic barriers for sediments, would also condition the axial transport of clastic sediments. In this context, the shallow marine deposits of the Peguera outcrops, with SW-W directed paleocurrents may have been the easternmost proximal equivalent of the early Eocene shallow marine facies of the Figols group in the Tremp syncline, as well as and the Baronia Fm. in the Ager syncline (Fig. 11 c). For this to happen, a pathway for clastics across the Montsec-Middle Pedraforca thrust front would be required. The lithic composition of La Baronia sandstones (De Rosa and Zuffa, 1979) includes metamorphic basement rocks indicating a Pyrenean source. Similarly, the detrital Zircons analysis (Thomson et al., 2020) indicates a Pyrenean-type source for these deposits. From Early Eocene to Lutetian times, platform carbonates developed south of the Ager basin. It is therefore difficult to figure out clastic systems sourced from the south (Ebro massif) flowing across these shallow marine carbonate platforms and feeding the Baronia Fm. in the Ager basin. In addition, growth strata geometries indicate that the rising Montsec front would prevent direct sediment flux from the northern hanging wall block, however we don't exclude the possibility of minor contribution from the hangingwall of the Montsec thrust (Fig. 11c). The most plausible possibility is that the clastics sediments

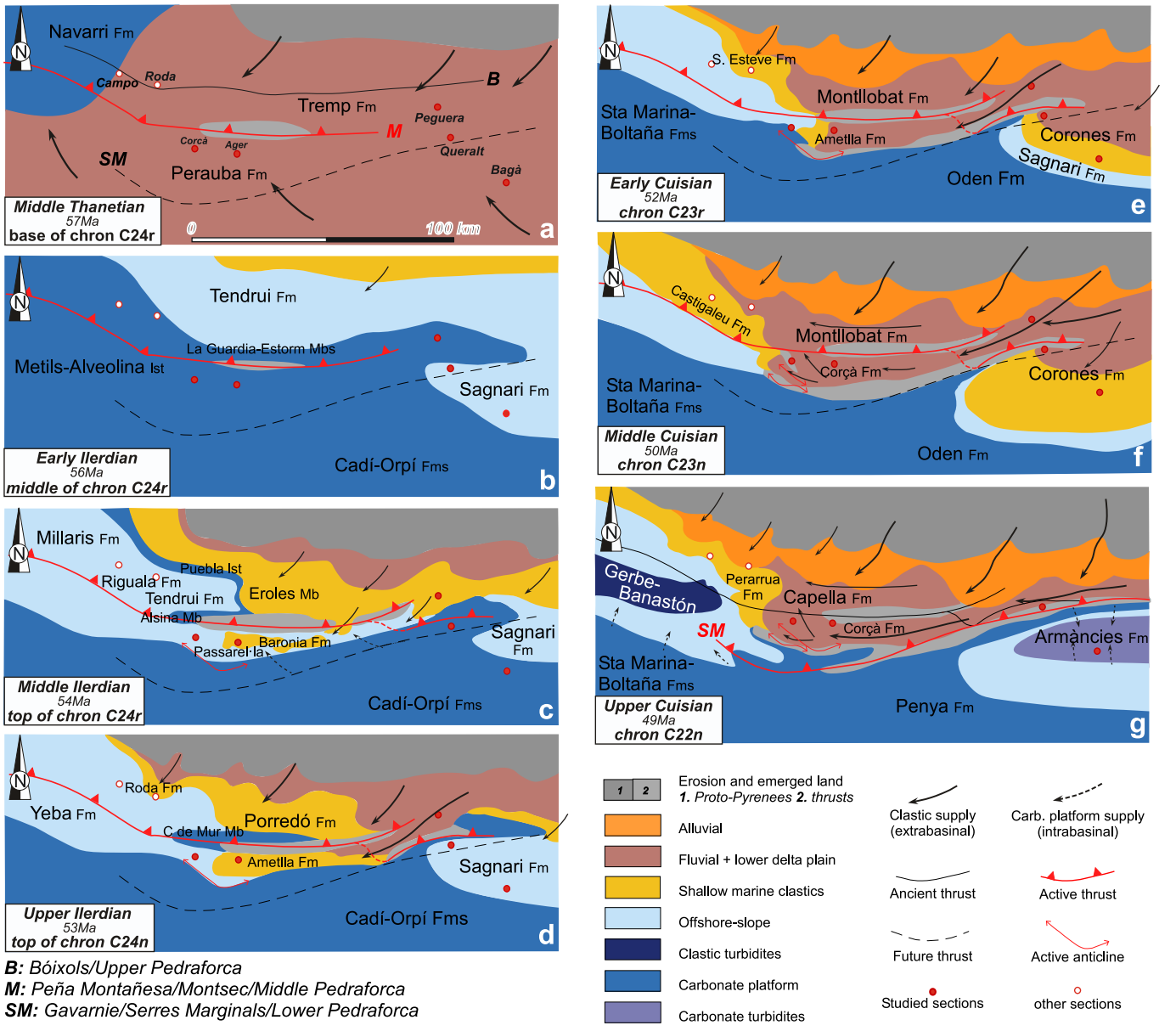

Fig. 11. Paleogeographic evolution of the South Pyrenean Foreland Basin. Based on Bentham and Burbank (1996), Betzler (1989), Cirés et al. (2007), Garcés et al. (2020), Juvany et al. (2024), Marzo et al. (1988), Molina et al. (1992), Muñoz et al. (2013), Nijman (1998), Picart et al. (2008, 2010a, 2010b, 2010c), Puigdefabregas et al. (1989), Serra-Kiel, et al. (1994). Tosquella (1995), Vergés (1993), Zamorano (1993), Solé Sugrañes and Clavell (1973).

crossed through the Montsec-Middle Pedraforca front through a low relief segment further East (transverse structure? Relay of structures?). This NE-SW clastic pathway would have been somewhere in between the Ager syncline and the Early Eocene outcrops of the Lower Pedraforca unit. Platform carbonates from the Cadí (including Port de Comte) and Pedraforca unit could have been the eastern factory of carbonates for the Baronia Fm mentioned as "carbonate shoals" in Olariu et al. (2012).

During the Cuisian, a generalized regressive trend is recorded by the Corones fluvial progradation (Ripoll) and the Passarella-Ametlla-Corçà (Ager) shallowing upwards sequence (Fig. 11d–g). Comparing the facies of time-equivalent fluvial systems from both areas, it is worth noting that the Corones Fm. represents a more distal environment (floodplains, fine-grained crevasse-splay and delta-plain deposits, and fine-grained channel fills) than the Corçà Fm. (coarse grained-conglomeratic fluvial channels and amalgamated sandstones). Paleocurrents indicate a SW-directed paleoflow for the Corones Fm., while in Corçà paleocurrents have a N and W direction (Nijman, 1998). Considering that the Corones outcrops are 100 km East from Corçà outcrops, it is not plausible that the fine-grained fluvial sediments of the Corones Fm. were the lateral equivalent proximal facies of the coarse-grained Corçà Fm. However, the chronology of both formations suggests a phase of enhanced sediment flux affecting the two sub-basins. This perturbation would have taken place in the proto-Pyrenees as evidenced by the detrital zircons signature (Odlum et al., 2019; Thomson et al., 2020) which indicates a similar "Pyrenean-type" source for both formations. As deduced from our observations, Corçà and Corones formations have a similar pyrenean source but represent two different routing systems. Corçà located to the north of middle pedraforca and running west through Àger basin and Corones filling the foreland south-east of middle Pedraforca. We don't have enough information to consider a unique routing system with an east provenance that diverged after the gowth of the middle Pedraforca structure.

5.2.4. *Sedimentation and subsidence rates*

Subsidence curves (Fig. 12) show a typical foreland basin sigmoidal shape with clear increasing to decreasing trend with maxima during

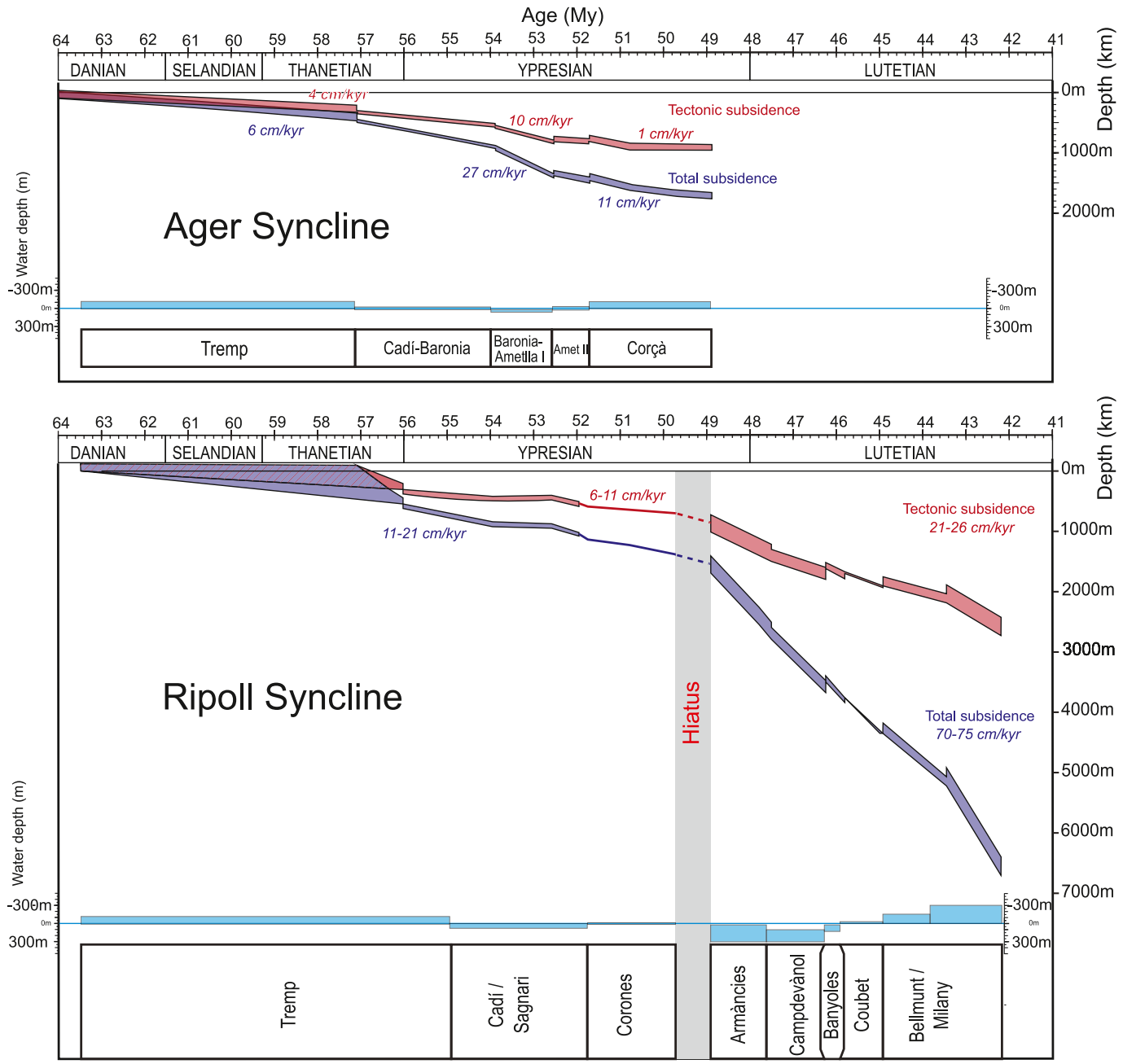

Fig. 12. Subsidence evolution of the composite sections from the Ripoll and Ager sub-basins.

C23r (Baronia to Ametlla I transition). Minimum (decompacted) sedimentation rates are 5 cm/kyr at times of the Tremp Fm., whereas maximum rates of 46 cm/kyr were reached at the Ametlla/Corçà transition. These values are in the same range as the ones obtained in the wedgetop and forebulge areas in Tremp-Graus Ainsa and Jaca basins (Vinyoles et al., 2021). As noticed in Tremp-Graus-Ainsa-Jaca basin, the transition from underfilled to overfilled accommodation (transition from marine to nonmarine) stands for a peak in sedimentation rates. When compared to the Ripoll basin (Juvany et al., 2024), Ager sedimentation rates are low, most notably during its foredeep stage.

Total and tectonic subsidence curves show the sigmoidal shape typical of foreland systems, with a first increasing and then decreasing subsidence trend. Initial total and tectonic subsidence rates in the Tremp Fm. are 6,17 cm/kyr and 4,32 cm/kyr respectively. Maximum values (reached at C23r and C24n) are 26,91 cm/kyr and 9,94 cm/kyr respectively and they evolve to lower values (11,35 cm/kyr Total and 1,03 cm/kyr Tectonic) to the upper part of the succession. Muñoz (2002) inferred a Paleocene-Early Eocene age for the Montsec Thrust emplacement and Middle Eocene to Oligocene for the Serres Marginals thrust sheet. This chronology places the Paleocene to Early Eocene filling of the Ager basin in a foredeep depozone. Thus, the observed subsidence evolution could be related to thrust kinematics. Increasing subsidence rates at middle Ilerdian were the flexural response to the emplacement of the Montsec thrust, the Ager basin undergoing a transition from forebulge-distal foredeep to foredeep. Decreasing subsidence at early Cuisian marks the evolution into a wedge top situation as the Serres Marginals thrusts start its emplacement. In Ripoll sub-basin there is a different and delayed history since it is in a different and more external tectonic unit. The passage from forebulge to foredeep (increasing rates at upper Cuisian) is associated to the initial emplacement of the Lower Pedraforca thrust sheet, equivalent to Serres Marginals in the Àger area. Maximum (foredeep) subsidence values are low

compared to other south-Pyrenean foredeep regions such as Ripoll and Jaca (Juvany et al., accepted; Vinyoles et al., 2021). Facies evolution shows that the Ager basin did not reach the deep-marine foredeep stage as Jaca or Ripoll. These facts show that the Montsec foredeep was a shallow and low-rate subsiding. This could be related to the massive salt migration towards the front of the Montsec thrust (Holl and Anastasio, 1993; Santolaria et al., 2016; Soto et al., 2002) which could partially counteract the regional subsidence. Others suggest that the Serres Marginals thrust activity started during the Early Eocene (Meigs, 1997). This would place the Ager basin in a wedge top setting in an early stage, justifying the moderate subsidence rates and the absence of a deep marine trough.

6. Conclusion

New magnetostratigraphic sections studied in the Ager syncline (South Central Pyrenees), spanning Paleocene to Early Eocene times are integrated with earlier magnetostratigraphic and marine-continental biostratigraphic data to produce a revised chronostratigraphy of the Paleogene sedimentary sequences of the Serres Marginals thrust sheet. The new chronostratigraphic framework allowed us to propose a well anchored correlation at the scale of the eastern-central Pyrenean foreland basin for the Late Paleocene-Early Eocene period. Integrated facies assemblages and paleocurrent observations from their equivalent units in the Lower and Middle Pedraforca have led to a detailed Early Eocene paleogeographic evolution of the Southern Pyrenean foreland.

Noteworthy in the evolution of the south Pyrenean foreland is the synchronicity of the evolution of Pyrenean sourced sedimentary systems during the Early Eocene, and of the development of stratigraphic cycles across the different sub-basins.

The post PETM sea-level rise at 55.5 My (Ilerdian marine flooding) contributed to a reorganization in the sediment routing by limiting the sediment flux from the southern iberian margin (Tremp Fm) and favoring the existing sediment flux from the emerging Pyrenees into the foreland (Baronia, Sagnari and Figols formations).

The Figols and Baronia formations were fed by sedimentary systems with SW, W and NW directed paleoflows, which developed onto the Middle-Lower Pedraforca Thrust Sheets, draining catchment areas of the eastern Pyrenees axial zone.

The fluvial systems of Castissent (Montsec Thrust Sheet) and Corçà (Serres Marginales Thrust Sheet) formations mark a pulse of sediment flux during the Cuisian that is coeval to the progradation of the Corones Fm. in the East but draining different catchment areas of the early Pyrenean massif.

A sigmoidal subsidence curve typical of flexural setting was obtained in the Ager syncline. Peak subsidence values, however, were modest and the Ager basin did not reach the deep-marine foredeep stage as occurred in the Jaca and Ripoll troughs. Salt migration during the Montsec thrust sheet emplacement and/or an early transition into a wedge-top position could have partially neutralized the regional subsidence.

CRediT authorship contribution statement

Philémon Juvany: Writing – review & editing, Writing – original draft, Investigation, Formal analysis, Data curation, Conceptualization. **Miguel Garcés:** Writing – review & editing, Visualization, Validation, Supervision, Resources, Funding acquisition, Data curation. **Miguel López-Blanco:** Writing – review & editing, Visualization, Validation, Supervision, Methodology. **Luís Valero:** Writing – review & editing, Visualization, Validation, Methodology, Investigation. **Elisabet Beamud Amorós:** Formal analysis. **Miquel Poyatos-Moré:** Investigation. **Albert Martínez Rius:** Investigation.

Declaration of competing interest

The authors declare that they have no known competing financial interests or personal relationships that could have appeared to influence the work reported in this paper.

Data availability

Data will be made available on request.

Acknowledgments

This is a contribution of the Marie Skłodowska-Curie Innovative Training Networks (H2020-MSCA-ITN-2019) Signal Propagation in Source to Sink for the Future of earth Resources and Energies (S2S-Future). Partially funded with Spanish project PID2019-106440 GB-C21/AEI/10.13039/501100011033) and Grup de Recerca reconegut per la Generalitat de Catalunya, 2021 SGR 00076 “Geodinàmica i Anàlisi de Conques”. We thank the Paleomagnetic Laboratory CCiTUB-Geo3BCN(CSIC) for the support on paleomagnetic analyses. This paper was greatly thanks to the comments of Emilio Pueyo-Morer and an anonymous reviewer.

Appendix A. Supplementary data

Supplementary data to this article can be found online at https://doi.org/10.1016/j.marpetgeo.2024.106913.

References

Badiola, A.Checa, Cuesta, M.A., Quer, R., Hooker, J.J., Astibia, H., 2009. The role of new Iberian finds in understanding European Eocene mammalian paleobiogeography. Geol. Acta 7, 243–258. https://doi.org/10.1344/105.000000281.

Beaumont, C., Muñoz, J.A., Hamilton, J., Fullsack, P., 2000. Factors controlling the Alpine evolution of the central Pyrenees inferred from a comparison of observations and geodynamical models. J. Geophys. Res. 105, 8121–8145. https://doi.org/10.1029/1999JB900390.

Bentham, P., Burbank, D.W., 1996. Chapter E 11: chronology of Eocene foreland basin evolution along the western oblique margin of the South-Central Pyrenees. In: Friend, P.F., Dabrio, C.J. (Eds.), Tertiary Basin of Spain. Cambridge University Press, pp. 144–152.

Betzler, C., 1989. A carbonate complex in an active foreland basin: the Paleogene of the Sierra de Port del Comte and the Sierra del Cadi (Southern Pyrenees). Geodin. Acta 3 (3), 207–220. https://doi.org/10.1080/09853111.1989.11105187.

Castelltort, S., Honegger, L., Adatte, T., Clark, J.D., Puigdefàbregas, C., Spangenberg, J. E., Dykstra, M.L., Fildani, A., 2017. Detecting eustatic and tectonic signals with carbon isotopes in deep-marine strata, Eocene Ainsa Basin, Spanish Pyrenees. Geology 45, 707–710. https://doi.org/10.1130/G39068.1.

Colombo, F., Cuevas, J.L., 1993. Características estratigráficas y sedimentológicas del "Garumniense" en el sector de Àger (Pre-Pirineo, Lleida). Acta Geol. Hisp. 28, 15–32.

Chanvry, E., Deschamps, R., Joseph, Ph, Puigdefàbregas, C., Poyatos-Moré, M., Serra-Kiel, J., Garcia, D., Teinturier, S., 2018. The influence of intrabasinal tectonics in the stratigraphic evolution of piggyback basin fills: towards a model from the Tremp-Graus-Ainsa Basin (South-Pyrenean Zone, Spain). Sediment. Geol. 377, 34–62. https://doi.org/10.1016/j.sedgeo.2018.09.007.

Checa, L., 2004. Revisión del género Diacodexis (Artiodactyla, Mammalia) en el Eoceno inferior del Noreste de España. Geobios 37, 325–335. https://doi.org/10.1016/j.geobios.2004.03.001.

Choukroune, P., 1989. The Ecors Pyrenean deep seismic profile reflection data and the overall structure of an orogenic belt. Tectonics 8, 23–39. https://doi.org/10.1029/TC008i001p00023.

Cirés, J., Samsó, J.M., Escuer, J., Saula, E., Cuevas, J.L., Mercadé, L., Arbués, P., Boix, C., Vilallonga, R., Caus, E., 2007. Mapa Geològic de Catalunya 1:2500. Calladrons 289 1-2 (63-24)/Sant Esteve de la Sarga 289 2-2 (64-24). Institut Geològic de Catalunya, Barcelona.

Crusafont, M., Rosell, J., Golpe, J.M., De Renzi, M., 1968. Le Paléogène de la vallée d’Ager et ses raports avec celui de la Conca de Tremp (Pyrénnées de la province de Lerida, Espagne). Mém. du B.R.G.M. 58.

De Rosa, R., Zuffa, G.G., 1979. Le areniti ibride della Valle di Ager (Eocene, Pirenei centro-meridionali) Mineralog. et Petrog. Acta 23, 1–12.

Dreyer, T., Fält, L.M., 1993. Facies analysis and high-resolution sequence stratigraphy of the Lower Eocene shallow marine Ametlla Formation, Spanish Pyrenees. Sedimentology 40, 667–697. https://doi.org/10.1111/j.1365-3091.1993.tb01355.x.

Ferrer, J., Le Calvez, Y., Luterbacher, H.P., Premoli Silva, I., 1973. Contribution a l’etude des foraminifères ilerdiens de la region de Tremp (Catalogne). Mem. du Museum d’Hist. Nat. n. série (C). 29, 1–107.

Fondevilla, V., Riera, V., Vila, B., Sellés, A.G., Dinarès-Turell, J., Vicens, E., Gaete, R., Oms, O., Galobart, A., 2019. Chronostratigraphic synthesis of the latest Cretaceous dinosaur turnover in south-western Europe. Earth Sci. Rev. 191, 168–189. https://doi.org/10.1016/j.earscirev.2019.01.007.

Galbrun, B., Feist, M., Colombo, F., Rocchia, R., Tambareau, Y., 1993. Magnetostratigraphy and biostratigraphy of cretaceous-tertiary continental deposits, Ager Basin, province of Lerida, Spain. Palaeogeogr. Palaeoclimatol. Palaeoecol. 102, 41–52. https://doi.org/10.1007/s10347-012-0317-1.

Garrido-Megias, A., 1973. Estudio Geológico y Relación Entre Tectónica y Sedimentación del Secundario y Terciario de la Vertiente Meridional Pirenaica en Su Zona Central (Provincias de Huesca y Lérida). PhD thesis. University of Granada.

Garcés, M., López-Blanco, M., Valero, L., Beamud, E., Muñoz, J.A., Oliva -Urcia, B., Vinyoles, A., Arbués, P., Cabello, P., Cabrer, Ll, 2020. Paleogeographic and sedimentary evolution of the south-Pyrenean foreland basin. Mar. Petrol. Geol. 113, 104105 https://doi.org/10.1016/j.marpetgeo.2019.104105.

García-Senz, J., Zamorano, M., 1992. Evolución tectónica y sedimentaria durante el Priaboniense superior-Mioceno inferior, en el frente de cabalgamiento de las Sierras Marginales occidentales. Acta Geol. Hisp. 27 (1–2), 195–209.

García, A., Ramírez Merino, J.L., Navarro, J.J., Ramírez del Pozo, J., Castaño, R., García-Senz, J., Leyva, f., Rodríguez, R., 2017. Memoria de la Hoja 328 (Benabarre). In: Mapa Geológico de España E. 1:50.000. Segunda Serie (MAGNA). IGME, Madrid.

Gradstein, F.M., Ogg, J.G., 2020. Chapter 2 - the chronostratigraphic scale. In: Gradstein, F.M., Ogg, J.G., Schmitz, M.D., Ogg, G.M. (Eds.), The Geologic Time Scale 2020, vol. 1. Elsevier, Amsterdam, pp. 21–32.

Grool, A.R., Ford, M., Vergés, J., Huismans, R.S., Christophoul, F., Dielforder, A., 2018. Insights into the crustal-scale dynamics of a doubly vergent orogen from a quantitative analysis of its forelands: a case study of the eastern Pyrenees. Tectonics 37, 450–476. https://doi.org/10.1002/2017TC004731.

Haq, B.U., Hardenbol, J., Vail, P.R., 1987. The phanerozoic record of global seasea-level change. Science 235, 1156. https://doi.org/10.1126/science.235.4793.1156.

Holl, J.E., Anastasio, D.J., 1993. Paleomagnetically derived folding rates, southern Pyrenees, Spain. Geology 21, 271–274. https://doi.org/10.1130/0091-7613.

Juvany, P., Garcés, M., López-Blanco, M., Martín-Closas, C., Beamud, E., Tosquella, J., Bekkevold, S., 2024. Chronostratigraphy and tectono-sedimentary history of the Eastern South-Pyrenean foreland basin (Ripoll syncline, NE Spain). The Depositional Record (in press).

Llompart, C., 1977. Paleoecología de la fauna de moluscos en un sector de la Vall d'Àger (prov. de Lleida). U.A.B. Publicaciones de Geologia 7. Barcelona.

Lopez-Mir, B., Muñoz, J.A., García Senz, J., 2014. Restoration of basins driven by extension and salt tectonics: example from the Cotiella Basin in the central Pyrenees. J. Struct. Geol. 69, 147–162. https://doi.org/10.1016/j.jsg.2014.09.022.

Luterbacher, H.P., 1969. Remarques sur la position stratigraphique de la formation d'Ager (Pyrenees Meridionals), vol. 69. Coll. sur l'Eocene, Mem, B.R.G.M., 255-232.

Luterbacher, H.P., 1973. La sección tipo del Piso Ilerdiense. In: XIII Congreso Europeo de Micropaleontología (España). ENADIMSA, pp. 113–140.

Martínez, A., Vergés, J., Muñoz, J.A., 1988. Secuencias de propagación del sistema de cabalgamientos de la terminación oriental del manto del Pedraforca y relación con los conglomerados sinorogénicos. Acta Geol. Hisp. 23, 119–128.

Martínez, A., Losantos, M., Domingo, F., Samsó, J.M., Saula, E., Soriano, C., Schöllhorn, E., Gisbert, J., Casas, J.M., Caus, E., 2020. Hoja nº 254 (Gósol), Mapa Geológico de España E. 1: 50.000. Segunda Serie (MAGNA). Instituto Geológico y Minero de España, Madrid.

Martinius, A., 2012. Chapter 18: contrasting styles of siliciclastic tidal deposits in a developing thrust-sheet-top basins-the lower Eocene of the central Pyrenees (Spain). In: Davis, R.A., Dalrymple, R.W. (Eds.), Principles of Tidal Sedimentology. Springer, pp. 473–506. https://doi.org/10.1007/978-94-007-0123-6_18.

Marzo, M., Nijman, W., Puigdefàbregas, C., 1988. Architecture of the castissent fluvial sheet sandstones, Eocene, south Pyrenees. Sedimentology 35, 719–738. https://doi.org/10.1111/j.1365-3091.1988.tb01247.x.

Mató, E., Martínez-Rius, A., Muñoz, J.A., Escuer, J., 1994. Hoja 293 (Berga). Mapa Geológico de España E. 1: 50.000. Segunda Serie (MAGNA). Instituto Geológico y Minero de España, Madrid.

Meigs, A.J., 1997. Sequential development of selected Pyrenean thrust faults. J. Struct. Geol. 19, 3–4.

Mencos, J., Carrera, N., Muñoz, J.A., 2005. Influence of rift basin geometry on the subsequent postrift sedimentation and basin inversion: the Organyà Basin and the Bóixols thrust sheet (south central Pyrenees). Tectonics 34, 1452–1474. https://doi.org/10.1002/2014TC003692.

Miller, K.G., Kominz, M.A., Browning, J.V., Wright, J.D., Mountain, G.S., Katz, M.E., Sugarman, P.J., Cramer, B.S., Christie-Blick, N., Pekar, S.F., 2005. The Phanerozoic record of global sea-level change. Science 310, 1293–1298. https://doi.org/10.1126/science.1116412.

Miller, K.G., Browning, J.V., John Schmelz, W.J., Kopp, R.E., Mountain, G.S., Wright, J. D., 2020. Cenozoic sea-level and cryospheric evolution from deep-sea geochemical and continental margin records. Sci. Adv. 6 (20) https://doi.org/10.1126/sciadv.aaz1346.

Minelli, N., Manzi, V., Roveri, M., 2013. The record of the paleocene-eocene thermal maximum in the Ager Basin (central Pyrenees, Spain). Geol. Acta 11, 421–441. https://doi.org/10.1344/105.000002061.

Molina, E., Canudo, J.L., Guernet, C., McDougall, K., Ortiz, N., Pascual, J.0., Pares, J., Samsó, J.M., Serra-Kiel, J., Tosquella, J., 1992. The stratotypic Ilerdian revisited: integrated stratigraphy across de Paleocene/Eocene boundary. Rev. Micropaleontol. 35 (2), 143–156.

Muñoz, J.A., 1992. Evolution of a continental collision belt: ECORS-Pyrenees crustal balanced cross-section. In: McClay, K.R. (Ed.), Thrust Tectonics. Springer, Netherlands, Dordrecht, pp. 235–246. https://doi.org/10.1007/978-94-011-3066-0_21.

Muñoz, J.A., 2002. The Pyrenees. In: Gibbons, W., Moreno, T. (Eds.), The Geology of Spain. Geol. Soc. of London, London, pp. 370–385.

Muñoz, J.A., Beamud, E., Fernández, O., Arbués, P., Dinarès-Turell, J., Poblet, J., 2013. The Ainsa Fold and thrust oblique zone of the central Pyrenees: kinematics of a curved contractional system from paleomagnetic and structural data. Tectonics 32 (5), 1142–1175. https://doi.org/10.1002/tect.20070.

Muñoz, J.A., Mencos, J., Roca, E., Carrera, N., Gratacós, O., Ferrer, O., Fernández, O., 2018. The structure of the South-Central Pyrenean fold and thrust belt as constrained by subsurface data. Geol. Acta 16, 439–460.

Mutti, E., Rosell, J., Allen, G.P., Fonnesu, F., Sgavetti, M., 1985. The Eocene Baronia tide dominated delta-shelf system in the Ager basin. In: Milà, M.D., Rosell, J. (Eds.), Excursion Guidebook, 6th European Regional Meeting. IAS, Lleida, pp. 579–600.

Mutti, E., Seguret, M., Sgavetti, M., 1988. Sedimentation and deformation in the Tertiary sequences of the southem Pyrenees. Field Trip Guidebook 7, A. A. P. G. Mediterranean Basins Conference.

Nijman, W., 1998. Cyclicity and basin axis shift in a piggyback basin: towards modelling of the Eocene tremp-ager basin, south Pyrenees, Spain. In: Mascle, A., Puigdefabregas, C., Luterbacher, H.P., Fernández, M. (Eds.), Cenozoic Foreland Basins of Western Europe, vol. 134. Geological Society Special Publications, pp. 135–162.

Odlum, M.L., Stockli, D.F., Capaldi, T.N., Thomson, K.D., Clark, J., Puigdefàbregas, C., Fildani, A., 2019. Tectonic and sediment provenance evolution of the South Eastern Pyrenean foreland basins during rift margin inversion and orogenic uplift. Tectonophysics 765, 226–248. https://doi.org/10.1016/j.tecto.2019.05.008.

Olariu, C., Steel, R.J., Dalrymple, R.W., Gingras, M.K., 2012. Tidal dunes versus tidal bars: the sedimentological and architectural characteristics of compound dunes in a tidal seaway, the lower Baronia Sandstone (Lower Eocene), Ager Basin, Spain. Sediment. Geol. 279, 134–155. https://doi.org/10.1016/j.sedgeo.2012.07.018.

Oms, O., J Dinarès-Turell, J., Vicens, E., Estrada, R., Vila, B., Galobart, A., Bravo, A.M., 2007. Integrated stratigraphy from the Vallcebre basin (southeastern Pyrenees, Spain): new insights on the continental cretaceous-tertiary transition in southwest europe. Palaeogeogr. Palaeoclimatol. Palaeoecol. 255, 35–47. https://doi.org/10.1016/j.palaeo.2007.02.039.

Picart, J., Saula, E., Samsó, J., Linares, R., Roqué, C., 2008. Mapa Geològic de Catalunya 1:2500. Àger 327 2-1 (64-25). Institut Geològic de Catalunya, Barcelona.

Picart, J., Saula, E., Samsó, J.M., 2010a. Mapa Geològic de Catalunya 1:2500. Os de Balaguer, 327–2–2. Institut Geològic de Catalunya, Barcelona, 64-26.

Picart, J., Samsó, J., Cuevas, J.L., Mercadé, L., Arbués, P., Barberà, X., Corregidor, J., López-Blanco, M., Salueña, I., Boix, C., Villalonga, R., Caus, E., Escuer, J., 2010b. Mapa Geològic de Catalunya 1:2500. Benavarri 289-1-1 (63-23)/El Pont de Montanyana, 289–2–1. Institut Geològic de Catalunya, Barcelona, 64-23.

Picart, J., Samsó, J., Cuevas, J.L., Mercadé, L., Arbués, P., Barberà, X., Corregidor, J., López-Blanco, M., Salueña, I., 2010c. Mapa Geològic de Catalunya 1:2500. Espills 251-2-2. Institut Geològic de Catalunya, Barcelona, 64-22.

PocovíJuan, A., 1978. Estudio geológico de las sierras Marginales Catalanas (Prepirineo de Lérida) Acta Geologica Hispanica, pp. 73–79.

Poyatos-Moré, M., Duller, R., Solé, X., Roda, D., Badia, A., 2013. Sediment routing and fluvial architecture in the ypresian-lutetian Corçà Fm (Àger basin, South-Central Pyrenees, Spain). In: 30th IAS Meeting of Sedimentology, Abstracts Volume, Manchester.

Puigdefabregas, C., 1975. La sedimentacion molasica de la Cuenca de Jaca. Pirineos 104–188.

Puigdefàbregas, C., Souquet, P., 1986. Tecto-sedimentary cycles and depositional sequences of the mesozoic and tertiary from the Pyrenees. Tectonophysics 129, 173–203.

Puigdefàbregas, C., Muñoz, J.A., Marzo, M., 1986. Thrust belt development in the Eastern Pyrenees and related depositional sequences in the southern Foreland Basin. In: Allen, P.A., Homewood, P. (Eds.), Foreland Basins. John Wiley & Sons, Ltd., pp. 229–246. https://doi.org/10.1002/9781444303810.ch12

Puigdefabregas, C., Collinson, J., Cuevas, J.L., Dreyer, T., Marzo, M., Mellere, D., Mercadé, L., Muñoz, J.A., Nijman, W., Vergés, J., 1989. Alluvial deposits of the successive foreland basin stages and their relation to Pyrenean thrust sequences. In: Fourth International Conference on Fluvial Sedimentology Guide-Book Series, 10. Sitges, Spain.

Puigdefàbregas, C., Muñoz, J.A., Vergés, J., 1992. Thrusting and foreland basin evolution in the Southern Pyrenees. In: Mc Clay, K. (Ed.), Thrust Tectonics. Springer, Dordrecht, pp. 247–254.

Rossi, C., 1997. Microcodium y trazas fósiles de invertebrados en facies continentales (Paleoceno de la Cuenca de Ager, Lerida). Rev. Soc. Geol. Espana 10 (3–4), 371–391.

Samsó, J.M., 1988. Estudi sedimentològic i bioestratigràfic de la Formació St. Esteve del Mall (Eocè, conca de Tremp-Graus). Masters Thesis. Universitat de Barcelona.

Santolaria, P., Casas-Sainz, A.M., Soto, R., Casas, A., 2016. Gravity modelling to assess salt tectonics in the western end of the South Pyrenean Central Unit. J. Geol. Soc. 174, 269–288. https://doi.org/10.1144/jgs2016-027.

Saula, E., Samsó, J.M., Escuer, J., Casanovas, J., 2017. Memoria de la Hoja 328 (Artesa de Segre). Mapa Geológico de España E. 1:50.000. Segunda Serie (MAGNA). IGME, Madrid.

Sclater, J.G., Christie, P.A., 1980. Continental stretching: an explanation of the post-mid-cretaceous subsidence of the central north sea basin. J. Geophys. Res. 85, 3711–3739. https://doi.org/10.1029/JB085iB07p03711.

Serra-Kiel, J., Canudo, J.I., Dinares, J., Molina, E., Ortiz, N., Pascual, J.0., Samsó, J.M., Tosquella, J., 1994. Cronoestratigrafía de los sedimentos marinos del Terciario inferior de la Cuenca de Graus-Tremp (Zona Central Pirenaica). Rev. Soc. Geol. Espana 7 (3–4), 273–297.

Serra-Kiel, J., Hottinger, L., Caus, E., Drobne, K., Ferrandez, C., Jauhri, A.K., Less, G., Pavlovec, R., Pignatti, J., Samsó, J.M., Schaub, H., Sirel, E., Strougo, A., Tambareau, Y., Tosquella, J., Zakrevskay, E., 1998. Larger foraminiferal

biostratigraphy of the tethyan Paleocene and Eocene. Bull. Soc. Geol. Fr. 169 (2), 281–299.
Serra-Kiel, J., Vicedo, V., Baceta, J.I., Bernaola, G., Robador, A., 2020. Paleocene larger foraminifera from the pyrenean basin with a recalibration of the Paleocene shallow benthic zone. Geol. Acta 18, 1–70. https://doi.org/10.1344/GeologicaActa2020.18.8.
Solé, F., Falconnet, J., Vidalenc, D., 2015. New fossil hyaenodonta (mammalia, placentalia) from the ypresian and lutetian of France and the evolution of the proviverrinae in southern europe. Palaeontology 58, 1049–1072.
Solé Sugrañes, L., Mascareñas, P., 1970. Sobre las formaciones Ager y Bagà, del Eoceno del Cadí Prepirineo oriental y de unos pretendidos olistolitos del mismo. Acta Geol. Hisp. 5, 97–101.
Solé Sugrañes, L., Clavell, E., 1973. Nota sobre la edad y posición tectónica de los conglomerados eocenos de Queralt (Prepirineo oriental, Prov. de Barcelona). Acta Geol. Hisp. 8, 1–6.
Soto, R., Casas, A.M., Sorti, F., Faccenna, C., 2002. Role of lateral thickness variations on the development of oblique structures at the western end of the South Pyrenean Central Unit. Tectonophysics 350, 215–235. https://doi.org/10.1016/S0040-1951(02)00116-6.
Souquet, P., 1988. Evolución del margen noribérico en los Pirineos durante el Mesozoico. Rev. Soc. Geol. Espana 1, 349–356.
Steckler, M.S., Watts, A.B., 1978. Subsidence of the Atlantic-type continental margin off New York. Earth Planet Sci. Lett. 41, 1–13. https://doi.org/10.1016/0012-821x(78)90036-5.
Speijer, R.P., Pälike, H., Hollis, C.J., Hooker, J.J., Ogg, J.G., 2020. Chapter 28: the Paleogene period. In: Gradstein, F.M., Ogg, J.G., Schmitz, M.D., Ogg, G.M. (Eds.), The Geologic Time Scale 2020. Elsevier, pp. 1087–1140. https://doi.org/10.1016/B978-0-12-824360-2.00028-0.
Tauxe, L., Shaar, R., Jonestrask, L., Swanson-Hysell, N.L., Minnett, R., Koppers, A.A.P., Constable, C.G., Jarboe, N., Gaastra, K., Fairchild, L., 2016. PmagPy: software package for paleomagnetic data analysis and a bridge to the magnetics information consortium (MagIC) database. G-cubed 17, 2450–2463. https://doi.org/10.1002/2016GC006307.
Teixell, A., 1998. Crustal structure and orogenic material budget in the west central Pyrenees. Tectonics 17, 395–406. https://doi.org/10.1029/98TC00561.
Teixell, A., Muñoz, J.A., 2000. Evolución tectonosedimentaria del Pirineo meridional durante el Terciario: una síntesis basada en la transversal del río Noguera Ribagorçana. Rev. Soc. Geol. Espana 13 (2), 251–264.
Teixell, A., Leyva, F., 2006. Memoria de la Hoja 327 (Os de Balaguer). Mapa Geológico de España E. 1:50.000. Segunda Serie (MAGNA). IGME, Madrid.
Teixell, A., Labaume, P., Lagabrielle, Y., 2016. The crustal evolution of the west-central Pyrenees revisited: inferences from a new kinematic scenario. C. R. Geosci. 348, 257–267. https://doi.org/10.1016/j.crte.2015.10.010.
Tosquella, J., 1988. Estudi sedimentològic i bioestratigràfic de la Formación Gresos de Roda (Eocè, conca de Tremp-Graus). Masters Thhesis. Universitat de Barcelona.
Tosquella, J., 1995. Els Nummulitinae del Paleocè-Eocè inferior de la conca sudpirinenca. Universitat de Barcelona. PhD Thesis.
Thomson, K.D., Stockli, D.F., Odlum, M.J., Tolentino, P., Puigdefàbregas, C., Clark, J.D., Fildani, A., 2020. Sediment provenance and routing evolution in the late cretaceous–eocene Ager Basin, south-central Pyrenees, Spain. Basin Res. 32, 485–504. https://doi.org/10.1111/bre.12376.
Tremblin, M., Khozyem, H., Adatte, T., Spangenberg, J.E., Fillon, C., Grauls, A., Hunger, T., Nowak, A., Läuchli, C., Lasseur, E., Roig, J., Serrano, O., Calassou, S., Guillocheau, F., Castelltort, S., 2022. Mercury enrichments of the Pyrenean foreland basins sediments support enhanced volcanism during the Paleocene-Eocene thermal maximum (PETM). Global Planet. Change 212, 103794. https://doi.org/10.1016/j.gloplacha.2022.103794.
Van Eeckhout, J.A., Giménez, J., Martínez, A., Mató, E., Ramos, E., Saula, E., Busquets, P., Colombo, F., Permanyer, A., 1991. Variaciones Geométricas de la cuenca de antepaís surpirenaica relacionadas con los episodios de progradación-retrogradación de los sistemas deposicionales aluviales transicionales y marinos en la zona del Ripollès-Berguedà. In: Colombo, F. (Ed.), I Congreso del Grupo Español del Terciario, Excursion Guidebook 3.
Van Hinte, J.E., 1978. Geohistory analysis - application of micropaleontology in exploration geology. AAPG Bull. 62 (2), 201–222. https://doi.org/10.1306/C1EA4815-16C9-11D7-8645000102C1865D.
Vergés, J., 1993. Estudi geològic del vessant sud del Pirineu oriental i central. Evolució cinemàtica en 3D. PhD Thesis Univ. Barcelona, Monografia Tècnica 7. Servei Geològic de Catalunya, Barcelona.
Vergés, J., Millan, H., Roca, E., Muñoz, J.A., Marzo, M., Cires, J., Den Bezemer, T., Zoetemeijer, R., Cloetingh, S., 1995. Eastern Pyrenees and related foreland basins: pre-, syn- and post-collisional crustal-scale cross-sections. Mar. Petrol. Geol. 12, 903–915. https://doi.org/10.1016/0264-8172(95)98854-X.
Vergés, J., Santaeulària, T., Serra-Kiel, J., Burbank, D.W., Muñoz, J.A., Giménez-Montsant, J., 1998. Quantified vertical motions and tectonic evolution of the SE Pyrenean foreland basin. Geol. Soc. Spec. Publ. 134, 107–134. https://doi.org/10.1144/gsl.sp.1998.134.01.06.
Vergés, J., Fernàndez, M., Martínez, A., 2002. The Pyrenean orogen: pre-, syn-, and post-collisional evolution. In: Rosenbaum, G., Lister, G. (Eds.), Reconstruction of the Evolution of the Alpine-Himalayan Orogen, vol. 8. J. Virtual Explor. https://doi.org/10.3809/jvirtex.2002.00058.
Vicente, A., Villalba-Breva, S., Ferràndez-Cañadell, C., Martín-Closas, C., 2016. Revision of the maastrichtian-palaeocene charophyte biostratigraphy of the fontllonga reference section (Southern Pyrenees, Catalonia, Spain). Geol. Acta 14 (4), 349–362. https://doi.org/10.1344/GeologicaActa2016.14.4.2.
Vinyoles, A., López-Blanco, M., Garcés, M., Arbués, P., Valero, L., Beamud, E., Oliva-Urcia, B., Cabello, P., 2021. 10 Myr evolution of sedimentation rates in a deep marine to non-marine foreland basin system: tectonic and sedimentary controls (Eocene,Tremp–Jaca basin, Southern Pyrenees, NE Spain). Basin Res. 33, 447–477. https://doi.org/10.1111/bre.12481.
Whitchurch, A.L., Carter, A., Sinclair, H.D., Duller, R.A., Whittaker, A.C., Allen, P.A., 2011. Sediment routing system evolution within a diachronously uplifting orogen: insights from detrital zircon thermochronological analyses from the south-central Pyrenees. Am. J. Sci. 311, 442–482.
Zamorano, M., 1993. Los Sistemas Deltaicos del Ilerdiense superior-Cuisiense de la Cuenca de Àger (Fm. Ametlla). Prepirineo de Lleida. PHD thesis. Universitat Autònoma de Barcelona.